Author Manuscript

Author Manuscript

Author Manuscript

Author Manuscript

HHS Public Access

Author manuscript

Adv Funct Mater. Author manuscript; available in PMC 2022 April 13.

Published in final edited form as:

Adv Funct Mater. 2021 February 03; 31(6): . doi:10.1002/adfm.202006796.

Bone-on-a-chip: microfluidic technologies and microphysiologic models of bone tissue

Amin Mansoorifar[1], **Ryan Gordon**[2], **Raymond Bergan**[2], **Luiz E. Bertassoni**[1,3,4,5,*]

[1]Department of Restorative Dentistry, School of Dentistry, Oregon Health & Science University, Portland, OR, USA.

[2]Division of Hematology/Oncology, Knight Cancer Institute, Oregon Health & Science University, Portland, OR, USA

[3]Center for Regenerative Medicine, School of Medicine, Oregon Health & Science University, Portland, OR, USA.

[4]Department of Biomedical Engineering, School of Medicine, Oregon Health & Science University, Portland, OR, USA.

[5]Cancer Early Detection Advanced Research Center (CEDAR), Knight Cancer Institute, Portland, OR, USA

Abstract

Bone is an active organ that continuously undergoes an orchestrated process of remodeling throughout life. Bone tissue is uniquely capable of adapting to loading, hormonal, and other changes happening in the body, as well as repairing bone that becomes damaged to maintain tissue integrity. On the other hand, diseases such as osteoporosis and metastatic cancers disrupt normal bone homeostasis leading to compromised function. Historically, our ability to investigate processes related to either physiologic or diseased bone tissue has been limited by traditional models that fail to emulate the complexity of native bone. Organ-on-a-chip models are based on technological advances in tissue engineering and microfluidics, enabling the reproduction of key features specific to tissue microenvironments within a microfabricated device. Compared to conventional *in-vitro* and *in-vivo* bone models, microfluidic models, and especially organs-on-a-chip platforms, provide more biomimetic tissue culture conditions, with increased predictive power for clinical assays. In this review, we will report microfluidic and organ-on-a-chip technologies designed for understanding the biology of bone as well as bone-related diseases and treatments. Finally, we discuss the limitations of the current models and point toward future directions for microfluidics and organ-on-a-chip technologies in bone research.

Graphical Abstract

Compared to conventional *in-vitro* and *in-vivo* bone models, microfluidic models and especially organs-on-a-chip platforms, provide more biomimetic tissue culture conditions, with increased

*Corresponding Author: bertasso@ohsu.edu, Tel: (503) 494-8763.

Conflict of Interest

The authors declare no conflict of interest.

Author Manuscript Author Manuscript Author Manuscript Author Manuscript

predictive power for clinical assays. In this progress report, microfluidic and organ-on-a-chip technologies designed for understanding the biology of bone as well as bone-related diseases and treatments will be covered.

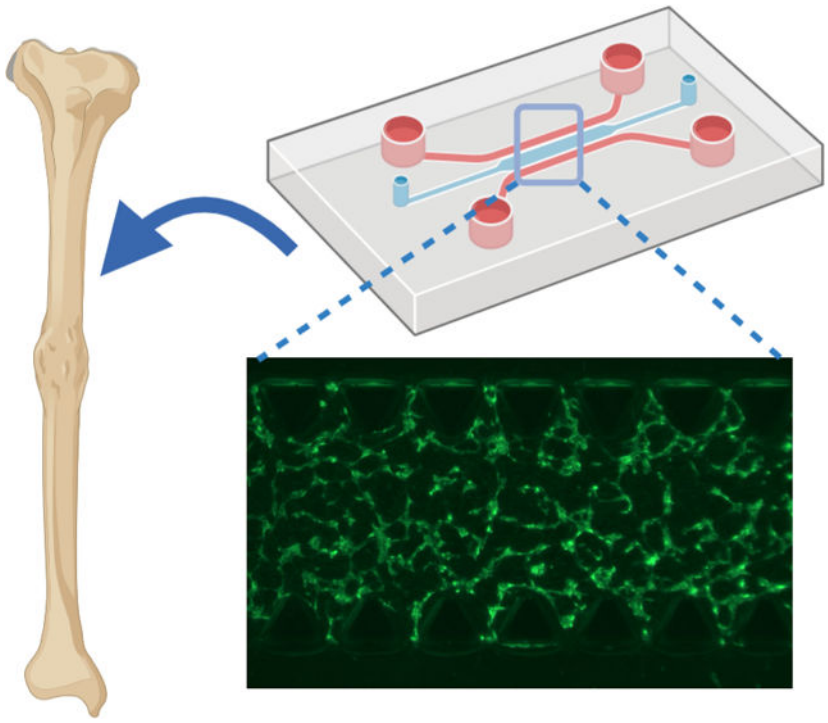

Keywords

bone; organ on-a-chip; microfluidic; cancer metastasis

1. Introduction

Bone is a highly mineralized tissue that performs essential functions in the body, such as locomotion, soft tissue structural support, hormone regulation, and bone marrow enclosure.[1–3] As such, bone can be characterized as a dynamic organ that is perpetually synthesized and resorbed by osteoblast and osteoclast cells during growth or injury.[4, 5] Osteocytes, another type of bone cells, are primarily responsible for orchestrating such a complex remodeling process in a paracrine manner.[6] Normal bone remodeling is critical in injury or fracture cases, and any imbalance of this orchestrated process can lead to severe bone diseases.[7, 8] The most common disease caused by elevated bone resorption is osteoporosis, affecting one in three women over 50 years old.[7] Existing data suggests that by 2025, osteoporosis will cause three million fractures and an annual economic burden of $25.3 billion.[9, 10] Another complication affecting bone tissue is due to metastatic cancer. Bone is the third most frequent site of metastasis and the most common metastasic site for breast, prostate, and lung cancer.[11] Additionally, other cancer types such as thyroid, kidney, and melanoma can also metastasize into bone.[11]

Author Manuscript Author Manuscript Author Manuscript Author Manuscript

Most studies investigating bone regeneration and cancer mediated bone destruction are conducted using conventional *in-vitro* two-dimensional (2D) cell culture systems or *in-vivo* animal models.[12–15] Conventional cell culture protocols provide the ability to study cell behavior using relatively cheap materials and simple technologies.[16] However, they lack the ability to replicate the 3D nature of the bone microenvironment, as well as many of the dynamic cell-cell and cell-matrix interactions that are necessary for physiological bone function.[17] On the other hand, animal models, despite providing a more physiological environment, lack the presence of human cells, limiting their relevance as predictive models of human tissue response.[18, 19] Even humanized murine cancer models fail to explicitly recapitulate the complex biology of the metastatic bone microenvironment.[20] Although many organs on a chip studies use animal cell lines, this technology allows the straightforward use of primary human cells, which have also been used extensively in the field.[21–23]

In order to overcome these difficulties, microfluidics has been proposed as a tool to mimic the physiological microenvironment of various tissues.[24–26] Microfluidics is a technology that processes or manipulates small amounts of fluids, using channels with dimensions ranging from tens to hundreds of micrometers.[27] Microfluidic devices provide opportunities such as high surface to volume ratio, presence of shear stress, and controllable chemical and physical gradients necessary for biological environments, which are inaccessible in macro-scale cell studies and uncontrollable in *in-vivo* studies.[28–31] Microfluidic models can recreate the biomimetic environment by culturing different cell types and tuning the spatiotemporal chemical and physical gradients and mechanical properties of the cellular microenvironment to create the so-called organ-on-a-chip platforms.[32–34] Altogether, this technology represents a platform for building human physiological models and investigating drug discovery and toxicology research.[35–38] During the last decade, organs-on-a-chip platforms have been widely used to mimic the physiological environment of different organs such as lung,[39, 40] kidney,[41, 42] heart,[43, 44] intestine,[45, 46] teeth,[47] and, bone. There have been many review papers concerning the development of the general topic of organ-on-a-chip, as well as specific platforms devoted to various organ systems in the literature.[32, 37, 41, 48–51] However, due to the higher complexity of the bone tissue compared to other tissues, microfluidic technologies and especially bone-on-a-chip platforms, have not yet been reviewed. Therefore, the current review addresses recent developments and challenges in the field to enable more efficient progress toward understanding bone physiology and diseases in microfluidic systems. To that end, we first describe the stages of bone formation and microfluidic devices developed to understand key bone biological processes. These include cell proliferation, differentiation, and interactions between osteoblasts, osteoclasts, and osteocytes, in both healthy and diseased bone tissue, along with the application of microfluidics in bone regeneration studies. We then review the progress made in vascularization and innervation of bone-on-a-chip organotypic model systems. We further discuss bone metastasis and the microfluidic devices designed to model the discrete stages of this process, as well as signaling pathways associated with it. Finally, we discuss the limitations of the current research and present insights for future directions.

Author Manuscript Author Manuscript Author Manuscript Author Manuscript

2. Microfluidics and organs-on-a-chip to study bone cell function

Bone tissue is composed of a cell-loaded mineralized matrix that is organized in a complex structural arrangement. The denser outer bone layer (cortical) and a spongy inner layer bone (trabecular) are both formed by the organization of mineralized collagen fibers, but in a significantly different microscale arrangement. Osteons are cylindrical features aligned parallel to the long axis of the bone and consist of lamellae. Lamellae are layers of compact matrix surrounding Haversian canals, which contain blood vessels and nerve fibers. Irrespective of the bone tissue type (trabecular or cortical), the presence of vasculature, innervation, along with resident bone cells (osteoblasts, osteoclasts, osteocytes) is what defines bone from a biologic standpoint. Osteoblasts are mesenchyme-derived mononuclear cells that form tight junctions with neighboring cells, and as they progress toward full differentiation from an osteoprogenitor phenotype to an osteocyte lineage, and are able to secrete different components of the bone matrix. Bone matrix synthesis begins with the secretion of osteoid tissue, followed by matrix mineralization and maturation resulting from complex biological processes that have been reviewed previously.[52, 53] After osteoid secretion, some of these specialized cells become embedded in the secreted matrix, which triggers their terminal differentiation into osteocytes, the most abundant cell type in bone tissue.[54–56] Proliferation, differentiation, and maturation of osteoblasts can be categorized into three main stages: (i) proliferation and extracellular collagen matrix formation, (ii) matrix maturation, proliferation decrease, and an increase in alkaline phosphate (ALP) activity, (iii) and finally a mineralization phase with a decrease in proliferation and ALP activity.[57, 58] *In-vitro* studies have shown that bone cells are responsive to various mechanical signals such as shear stress, hydrostatic pressure, and substrate deformation.[12, 59–61] Specifically, shear stresses experienced by osteoblasts have been reported to impact biochemical factors as well as intracellular messengers and transcription factors.[12, 62]

Microfluidic devices can facilitate the development of culture conditions that more closely emulate the *in-vivo* environment of these biological processes than conventional 2D cell cultures. This can be achieved by developing microdevices that allow for fluidic and spatially-defined control of oxygen and nutrient delivery to the cells, increasing concentration of metabolites and secreted factors, and controlled application of mechanical stimulation to cells or tissues in the device.[63] Precise flow control using a syringe pump, peristaltic pumps, or pressure-control systems is a key parameter in controlling the shear stress exerted on biological systems. For instance, a microfluidic device was developed to study the effects of shear stress on bone-forming cells cultured on fibrous collagen.[64] The device was composed of a microchamber connected to a pressure pump to induce precise pressure drops and flow rates to the system (Figure 1A). The results showed that MC3T3-E1 pre-osteoblastic cells cultured on a collagenous substrate in the microfluidic device exposed to a flow rate of 50 μL/min (0.5 dyn/cm^2 shear stress) experienced a 2.4-fold increase in cell proliferation compared to static conditions. However, 30 μL/min (0.3 dyn/cm^2 shear stress) flowrate just slightly increased the proliferation without significant difference compared to the static culture. On the other hand, the ALP activity of the cultured cells had a 1.6-fold increase in 30 μL/min, whereas, in the flow rate of 50 μL/min, ALP activity was not

Author Manuscript Author Manuscript Author Manuscript Author Manuscript

significantly increased. The differences seen in this report were attributed to the increased proliferation under higher flow rate due to enhanced nutrient transport, which promotes maturation to the later stages of the osteoblastic phenotype with decreased ALP activity.

Osteocytes use the extension of their plasma membrane to communicate with one another, as well as with osteoclasts.[65, 66] Osteoclasts are large multinucleated cells stimulated by osteocytes and osteoblasts to absorb the bone tissue during growth and remodeling.[3] Differentiation, activation, or apoptosis of bone cells (osteoblasts, osteocytes, and osteoclasts) are often dependent on intracellular communication between all bone cell types through ligand-receptor communications and molecules and ions traveling in the extracellular matrix (ECM) or gap junctions.[67–69] Osteocyte mechanotransduction and cell regulation studies are mostly based on macroscopic scale parallel plate flow chambers (PPFC).[70, 71] However, due to the large size of these chambers, difficulties such as lack of real-time signaling, unidirectional signaling, and large number of primary osteocytes arise. In order to solve these problems, a microfluidic platform was developed by Middleton *et al.* to study the bone cell-cell communications at physiologically relevant distances (Figure 1B).[72] This platform was used to investigate the role of osteocytes and osteoclasts and their crosstalk in pathogenic diseases of the bone, such as osteoporosis and bone metastasis. The microfluidic device consisted of two or three channels separated by high resistance posts (Figure 1B). RAW264.7 (osteoclast precursor) cells were seeded in one channel while the other channel had a 1 μl/min perfusion of RAW media or RAW media supplemented with 50 ng/ml RANKL. Receptor activator of nuclear factor kappa-B ligand (RANKL), a member of the tumor necrosis factor (TNF) cytokine family, is expressed by osteoblasts and results in recruitment of, maturation, differentiation, and activation of osteoclasts through binding to the RANK receptor.[73, 74] When RANKL supplemented RAW media was perfused into the system, cells preferentially increased density toward the RANKL source, and multinucleated cells began to form within 600 μm of the RANKL source (Figure 1C). After that, the osteoclast precursors were simultaneously exposed to mechanically-stimulated and non-stimulated MLO-Y4 osteocytes on both sides. The stimulated osteocytes underwent daily fluid shear stress of 1 Pa for 1 hour. The results showed an increased precursor density toward the non-stimulated channel (Figure 1D). The authors suggested that such an increase was due to the fact that RANKL expression is higher in non-stimulated MLO-Y4 cells, therefore attracting the precursors. Furthermore, TRAP+ (a marker of osteoclast maturation) multinucleated cells proved osteoclastogenesis within 200 μm of the non-stimulated channel (Figure 1D). In order to better characterize the osteoclastogenesis, the ratio of RANKL to osteoprotegerin (OPG) is usually used. OPG is another member of the TNF receptor family that interrupts the signaling between osteoblasts and osteoclast progenitors and acts as a decoy receptor to RANKL.[73–75] This ratio is decreased by mechanical stimulation leading to a poorer differentiation.[73–75] Non-stimulated osteocytes will undergo apoptosis, which will increase RANKL expression and decreased expression of OPG, which will promote osteoclast differentiation.[73–75] In another experiment, MLO-Y4 cells exposed to mechanical stimulation were seeded in an adjacent channel containing either RAW264.7 cells with 10 ng/ml RANKL supplemented RAW media or MLO-Y4 cells. The results showed a higher calcium response when osteocytes were co-cultured with osteoclasts compared with co-culturing with osteocytes (71 ± 14% compared to 33 ± 7%).

Author Manuscript Author Manuscript Author Manuscript Author Manuscript

One particular factor secreted by osteoclasts that can affect osteocyte mechanosensitivity is sphingosine-1-phosphate (S1P).[70, 76, 77] Inhibition of sphingosine kinases in MLO-Y4 osteocytes have been shown to decrease the percentage of responding cells undergoing oscillatory fluid flow *in-vitro*.[70]

3. Microfluidics for bone regeneration and tissue engineering

Regenerative medicine strategies, involving the combination of biomaterials/scaffolds, cells, and bioactive agents, have been employed extensively for bone repair and regrowth.[78] While the field of organs-on-a-chip has evolved to develop model systems aimed at studying physiologic and disease processes, microfluidics has also been utilized to accelerate the development of biomaterials for regenerative applications, as well as to develop miniaturized and high-precision bioreactors.[79–81] For instance, a simple high-throughput microfluidic platform was developed to study the efficacy of biomaterials aimed at accelerating wound healing and preventing bacterial infection (Figure 2A).[82] In the referred study, inkjet-printed antibiotic and calcium-eluting micropatterns were formed in a microchannel for high-throughput studying of the beneficial effects of antibiotics on bacterial killing without the adverse effects on osteoblastic tissue formation, and the positive effects of biphasic calcium phosphate (BCP) patterns on osteogenic tissue development. The results show that when RFP and BCP were not used in the ink mixture, the release of live bacteria was detected around day 2 when the chambers were previously inoculated with S. epidermidis. The number of bacteria was increased exponentially by day 3 and reached a steady-state of 10^8 CFU/ml (Figure 2B). The UV/VIS results showed that the chambers become acidic (Figure 2B), and osteoblasts appeared unhealthy and detached from the surface by day 9. However, by using RFP containing inks, no planktonic bacteria nor biofilm colonies were observed (Figure 2B). Moreover, the results revealed that BCP containing inks produced about two times more calcium and promoted osteogenic development (Figure 2C).

Cell migration is another critical step in many regenerative processes, including bone regeneration. 3D cell migration can be either proteolytic or non-proteolytic.[83] In proteolytic migration, cells secrete active metalloproteases to break down ECM for movement while in non-proteolytic migration, cells deform the ECM or squeeze through it.[83] The migration of highly motile cells, such as fibroblasts, has been extensively investigated.[84, 85] However, the favorable migration behavior of human osteoblasts in an osteoid-like collagenous matrix has remained elusive. Using microfluidics technology, 3D migration of human osteoblasts in a model of bone injury or fracture was investigated (Figure 2D).[86] In this study, a collagen-based hydrogel was altered by crosslinking with Transglutaminase (TG2) to increase its strength as well as its resistance to proteolytic digestion. In order to recreate the physiological environment of the bone fracture or injury, a chemical gradient of platelet-derived growth factor (PDGF-BB), which plays a significant role in the directed migration of osteoblasts, was applied across the gel. The addition of TG2 increased the number of thin membranes between fibers and caused a more aligned architecture. The results show that although TG2 causes resistance to proteolysis, human osteoblasts can still degrade the ECM for their movement. Based on the results, high concentrations of chemoattractant induces an inhibitory effect to reduce the cell velocity while the lower concentrations increased the cell's speed. However, by using MMP

Author Manuscript Author Manuscript Author Manuscript Author Manuscript

inhibitors, the mean and effective speeds of cells drastically decreased (Figure 2E). The same reduction was observed in the calculated diffusion coefficients proving the critical role of MMP for the human osteoblast movement.

In another set of studies, microfluidic devices were used to investigate processes related to bone erosion resulting from an imbalance between osteoclast bone resorption and osteoblast bone formation. The main trigger of articular bone erosion is fibroblast-like synoviocytes (FLS), populating the intimal lining of the synovium that produces proinflammatory cytokines and receptor activators of RANKL.[87–89] A microfluidic device having six parallel branched microchannels that are joined at the cell reservoir at one end and joined at the center channel on the other end was used to study the FLS migration happening with rheumatoid arthritis (RA) and the clinical strategy for its treatment (Figure 2F).[90] In order to mimic FLS migration in RA, human synovium SW982 cells were cultured in the central channel, while RAW264.7 RANKL stimulated cells and osteogenic medium stimulated bone marrow-derived mesenchymal stem cells (BMSCs) cells were cultured on the side chamber (Figure 2G). The results revealed an increased number of migrated FLS cells and distance when BMSCs and RAW264.7 cells were co-cultured compared to monocultures. Moreover, migrated FLS showed high levels of cadherin-11 expression, which promotes the secretion of inflammatory factor IL-6 responsible in the activation and migration of FLS. The results also showed an increase of TRAP+ RAW264.7 cells showing higher osteoclastic activity while the number of ALP staining positive cells decreased, which indicates an inhibition in osteoblastic differentiation. They also tested Celastrol's effectiveness in treating RA by adding 500 ng/ml Celastrol to the co-culture and incubated for 4 days. Adding Celastrol decreased the number of migrated FLS, expression of cadherin-11, as well as the number of TRAP+ RAW264.7 staining cells. Celastrol inhibited FLS migration by suppressing HIF-1a/CXCR4 signaling pathway or TLR4/NF-kB-mediated MMP-9 expression, as recently shown in the literature.[91, 92]

4. Bone vasculature and innervation on-a-chip

Bone is a highly vascularized tissue with 10–15% of total cardiac circulatory output.[93, 94] Blood vessels in bone are responsible for exchanging oxygen, nutrients, and waste as well as providing bone with hormones, growth factors, and neurotransmitters necessary for bone cells' survival and activity.[95] Endothelial cells (EC), as the building blocks of the circulatory system, have been integrated into many microfluidic systems to recreate a more physiologically relevant system.[96, 97] We presented a 3D micromolding technique combined with EC cell lining technique to embed functional and perfusable microvessels inside various hydrogels and showed that the fabricated vascular network is efficient in improving mass transport and viability and differentiation of osteogenic cells in cell-laden GelMA hydrogels.[98] In contrast to the EC cell lining technique, vasculogenesis and angiogenesis-based methods can be combined with advanced microfluidic-based techniques to recreate 3D microvascular networks that can be adapted into organ-on-a-chip platforms.[99–105] A tri-culture of human bone marrow mesenchymal stem cells (hBM-MSCs), osteogenically differentiated (OD) hBM-MSCs, and human umbilical vein endothelial cells (HUVECs) embedded in 2.5 mg/ml fibrin gel were used to recreate the bone microvasculature.[106] Experimental results showed the formation of functional

Author Manuscript Author Manuscript Author Manuscript Author Manuscript

microvascular networks after 4 days. Positive alpha smooth muscle actin (SMA) staining and hBM-MSCs wrapping around microvessels showed the phenotypic adaption of hBM-MSCs toward a mural cell lineage (Figure 3A). Vasculature specific markers, such as vascular endothelial (VE)-cadherin and zonula occludens (ZO)-1, support the existence of mature vessel walls and tight cell junctions (Figure 3A). The secretion of bone proteins, such as osteocalcin and bone ALP, also supports the formation of mature bone tissue (Figure 3A). Furthermore, ECs showed morphological features such as elongated shape similar to *in-vivo* vasculature.

Organ innervation has been modeled using several microfluidic devices.[107–109] Like most other musculoskeletal tissues, bone is innervated by peripheral nerves, which coordinate with the central nervous system.[110, 111] The factors produced by nerve fibers have been directly associated with the activity of the bone cells.[110] In order to study the role of innervation in skeletal development, bone remodeling, and regeneration, a microfluidic device was developed to investigate the effects of dorsal root ganglion (DRG) neurons on the ability of MSCs to differentiate into osteoblasts.[112] The microfluidic device consisted of two parallel channels separated by several microgrooves adopted from previous neuron studies (Figure 3B). This unique design is beneficial to separately culture neuron bodies, and target cells with specialized culture media and measure the distinct gene/protein profiles of the neuron and target cells. DRG neurons and MSCs were cultured on the somal and axonal sides of the microdevice, and MSCs were seeded with osteoinductive medium (OIM). After 4 days of co-culture, neurites were detected within the axonal side of the microdevice (Figure 3C). The results revealed 40% and 55% increase in MSCs' metabolic activity on days 4 and 7 compared to the monoculture condition, respectively. Moreover, a 2.5-fold increase in RUNX2, a 2.8-fold increase in Sp7 (both RUNX2 and Sp7 play a significant role in directing the MSCs differentiation to osteoblasts and eventually osteocytes), a 2-fold increase in Col1α1 (expressed from the beginning of osteoblast differentiation and is the main structural component of bone matrix), and 3.4-fold increase in Bglap (a highly abundant bone protein secreted by osteoblasts) expression was seen in the co-culture condition. However, if MSCs were not cultured in an osteogenic medium, no differences in osteoblast-related genes between monoculture or co-culture were detected. These results showed the promotion of the osteogenic activity of MSCs due to DRG neurons during osteoblasts differentiation. Moreover, Cx43 levels, as the most abundant connexin in bone cells regulating direct cell-cell communications via gap junctions, reached maximum levels by day 4 of co-culture, which proved the positive impact of DRG neurons on MSCs during osteogenesis. The results also demonstrated the role of DRG neurons in increased N-cadherin levels in MSCs, which mediates cell-cell adhesions.

5. Cancer metastasis to bone

Cancer metastasis is a complex multistage process, including cell shedding from the primary tumor site, local invasion, intravasation to the local blood or lymphatic vessels, circulation through the bloodstream or lymphatic vessels, extravasation into the secondary site, the formation of micro and macro metastasis in the secondary organ, and the genesis of new blood vessels (angiogenesis) to provide oxygen and nutrients.[113, 114] A significant number of studies focusing on cancer metastasis utilize mouse models, wherein cells are either

Author Manuscript Author Manuscript Author Manuscript Author Manuscript

injected into circulation or orthotopically into the site of interest.[115, 116] Although *in-vivo* models provide a more physiologically relevant environment compared to conventional *in-vitro* models, for the most part, they fail to account for the impact of an intact immune system, especially in the context of the immunocompromised animals. While humanized mouse models exist, they are exceedingly expensive and still fail to completely recapitulate the human immune system, and as such, not widely deployed.[117] Moreover, the inherent phenotypic and genotypic differences that exist between animal and human cells represents another challenge. Microfluidic systems represent a powerful platform for the study of cancer metastasis by allowing for the co-culture of human cells as well as immune cells, closer emulating the native microenvironment in humans, coupled with inline, real-time, and high-throughput measurement capabilities.[118] Microfluidic systems and, in particular, organ-on-chip systems have been widely used to study metastatic processes such as invasion,[119, 120] intravasation,[121–123] extravasation,[123, 124] and angiogenesis[122, 125] in different human organs. However, the studies focusing on bone cancer metastasis are limited due to the relatively recent introduction of the bone-on-a-chip platform compared to other organ-on-chip systems.

Cell invasion is one of the early steps of cancer metastasis. In order to study the invasive behavior of prostate cancer cells, a microfluidic device equipped with multiphoton flavin adenine dinucleotide (FAD) analysis was used to study prostate cancer cells, LNCaP and C4–2B, co-cultured with murine calvarial pre-osteoblast cells (MC3T3-E1s).[126] Combining imagining techniques with microfluidics is an advantageous way of observing and extracting information from biological samples.[127] In the aforementioned device, after adhesion of MC3T3-E1 cells to the sides of the channels, the channels were coated with a thin layer of collagen type I, then prostate cancer cells were introduced to the channels, and their migratory/invasive behavior was studied. C4–2B cells showed an increase in the number of cellular protrusions when they were co-cultured with MC3T3-E1 cells compared to its monoculture. However, no difference was observed for LNCaP cells. This behavior was attributed to the androgen-dependent behavior of LNCaP cells, making them less invasive towards stromal cells, while androgen-independent C4–2Bs demonstrated more invasive behavior. The results also revealed that when C4–2Bs were treated with conditioned media from a mixture of C4–2Bs and MC3T3-E1s, the percentage of the protrusive C4–2Bs was markedly increased, due to the crosstalk interactions between cancer cells and stromal cells. Together the results demonstrate the capabilities of microdevices to study and quantify the crosstalk between a metastatic prostate cancer cell line and bone stromal cells.

Another process that has been extensively studied using microfluidics is the extravasation of the cancer cells. During extravasation, cancer cells must first migrate through the capillaries or lymphatic vessels and then invade the tissue matrix through the ECM by either changing its structure or through the pores within the ECM.[128] Mei *et al.* developed a microfluidic device to investigate the role of osteocytes in the mechanical regulation of breast cancer cell extravasation.[129] HUVECS were seeded on one of the channels, and an ellipsoidal lumen was formed, with consistent VE-cadherin expression after 6 hours. The effects of osteoclast-derived released factors on cancer cell extravasation was investigated by seeding MLO-Y4 cells in osteocyte channel with either MLO-Y4 media or 1:1 mixture of MLO-Y4 media and osteoclast conditioned media. The introduction of osteoclast-conditioned

Author Manuscript Author Manuscript Author Manuscript Author Manuscript

media did not change the extravasation percentage. However, the extravasated distance increased from 63.8 μm to 134.5 μm with the conditioned media. Osteoclasts are known to stimulate cancer metastasis through the breakdown of bone matrix (thereby releasing growth factors) and the direct secretion of osteoclast signals.[130, 131] In the absence of bone matrix resorption, studies have shown that deproteinized osteoclasts conditioned media and lipids extracted from osteoclasts conditioned media to promote cancer migration through the upregulation of arachidonic acid and the downregulation of lysophosphatidylcholine.[132] Also, sphingosine 1 phosphate (S1P) is secreted by osteoclasts and is known to promote breast cancer migration by upregulating matrix metalloproteinase (MMP)-9, which breast cancer cells utilize to degrade ECM.[133–135] However, S1P also can enhance endothelial integrity, thereby inhibiting the extravasation of breast cancer cells.[136] Similarly, the breast cancer cell line, MDA-MB-231, extravasated farther via increased matrix degradation, while the percentage of extravasation is still comparable between conditions due to the protection of the endothelium barrier.

In the same study, MLO-Y4 osteocytes underwent daily fluid stimulation of 1Pa and 1Hz for 2 hours to investigate the effects of mechanically stimulated osteocytes on breast cancer extravasation. The result revealed the reduction in extravasation percentage (33.8% compared to 67.2%) and distance (36.6 μm compared to 110.3 μm) compared to samples with no stimulation. Mechanically-stimulated osteocytes are known to increase adenosine triphosphate (ATP) secretion, through activation of gap junction hemichannels, and decrease RANKL release, which could both inhibit breast cancer migration.[137–140] Furthermore, the application of flow reduces osteocyte apoptosis, which reduces IL-6 expression, a factor that stimulates cancer cell expression of MMP's.[141, 142] However, mechanical stimulation also upregulates prostaglandin E2 (PGE-2) and TGF-β1 in osteocytes, both of which have been implicated in promoting metastasis through the increase of MMP expression in various cancers.[70, 143, 144] In terms of extravasation percentage, they suggested that the trend is due to PGE-2 secretion by mechanically stimulated osteocytes that will enhance the endothelial barrier and reduce its permeability. The ability of microdevices to control both mechanical stimulation and flow rates, as well as the establishment of an endothelial barrier adjacent to a bone-cell rich matrix, makes microfluidics a desirable alternative for studies on cancer metastasis.

It has long been recognized that cancer cells spread to specific distant organs.[145] Based on the "seed and soil theory" proposed by Paget, the cells (seeds) can only accomplish metastasis if the distant organ microenvironment (soil) is suitable for their growth.[146] This shows that the colonization, proliferation, and eventual outgrowth of the cancer cells are significantly related to the interactions between the cellular and physiochemical components of both cancer cells and the host organ environment. One of the widely used microfluidic devices to recreate organ tissues *in-vitro* was developed by Roger Kamm's group.[147, 148] This microfluidic device consists of a central gel channel separated from side medium channels by a novel post design, which allows the hydrogel to be contained within the channel during the gel filling process (Figure 4A).[106] Moreover, the gas-permeable laminate layer underlying the chips ensures that atmospheric oxygen and CO_2 levels are maintained. Whereas, concentration gradients and interstitial flows across the gel channel could also be recreated by applying different concentration solutions or flow rates to the

Author Manuscript Author Manuscript Author Manuscript Author Manuscript

side channels.[149, 150] This technology was deployed in a bone-on-chip study, where the gel channel was filled with 6 mg/ml collagen type I embedded with osteogenically differentiated (OD) hBM-MSCs cells. After 1 day, HUVECs cells were introduced to one of the medium channels to form a monolayer (Figure 4B).[106] Results demonstrated that OD cells were able to deposit calcium and produce mineralization of the surrounding matrix. VE-cadherin staining was used to confirm the tight connections between endothelial cells (Figure 4C), and laminin and collagen IV presence was used to show the presence of a mature endothelium. Finally, alizarin red staining showed the calcium deposited by OD hBM-MSCs (Figure 4D). In a similar approach, Bersini *et al.* used a bone-on-a-chip device to measure 70 kDa fluorescent dextran's permeability through a bone mimicking environment and acellular environment. Breast, bladder, or ovarian cancer cells (MDA-MB-231, T24, and OVCAR-3) were also introduced to the microdevice to study extravasation through an engineered endothelial barrier into the bone mimicking environment.[151] A significant increase in the extravasation rate of MDA-MB-231, T24, and OVCAR-3 with the presence of bone mimicking environment (64.3 ± 2.9%, 66.9 ± 3.5%, and 50.9 ± 2.2% respectively) compared to the acellular model (17.0 ± 4.7%, 16.0 ± 4.5%, 12.9 ± 3.6% respectively) was observed. The percentage of transmigrated cells in the case of MDA-MB-231 and T24 were significantly higher with respect to OVCAR-3, while there was no significant difference for all three cells in the acellular model. Additionally, the migration distances were calculated, and an increased migration distance in the bone mimicking environment compared to the acellular environment was observed. Moreover, it was observed that T24 cells migrated significantly more than other cell lines. These results indicate an aggressive behavior of T24, which makes it transmigrate through the endothelium and migrate considerable distances to the bone mimicking environment. Although clinical studies suggest that only 0.82% of ovarian cancer cells metastasize to bone,[152] the results here show more than 50% transmigration to the bone mimicking environment. The authors hypothesized that ovarian cancer cells, after extravasating to the bone environment, may not be able to form micrometastatic colonies.

In addition to seeding osteoblasts in a hydrogel, it is also possible to recreate the 3D bone environment through the active secretion of collagen by osteoblasts, followed by the deposition of HAP onto the structure over an extended period of time.[153] For example, a microfluidic system was developed for the secretion of a heavily mineralized osteoblastic tissue in 720 hours.[154] This microfluidic device consists of two chambers separated by a dialysis membrane (Figure 4E). The height of the cell culture chamber and dialysis pore size was optimized using numerical simulations. High pore size membranes were shown to be favorable because of the high exchange efficiency of nutrients and waste, while smaller pore size acted to block the translocation of bone-building proteins to the outside. On the other hand, the height determines the distance traveled by nutrients and waste as well as the local concentration of the bone-building proteins inside the cell chamber. The numerical simulations revealed that 2 mm cell chamber height with regenerated nitrocellulose (NC) dialysis membrane (pore size of 1.5 nm) would make a stable physiological environment that can exchange nutrients and waste while efficiently blocking the bone-forming proteins. They also generated nanostructures on the glass surface using a base wash with 0.3 M sodium hydroxide in 70% ethanol for 72 h to enhance osteoblastic tissue attachment.

Author Manuscript Author Manuscript Author Manuscript Author Manuscript

Murine calvaria pre-osteoblasts MC3T3-E1 were introduced into the culture chamber. After 720 h of culture, the thickness of the collagenous matrix reached an average of 60 μm, demonstrating the microfluidic device's ability to form a mature osteoblastic tissue. TEM horizontal view images of the osteoblastic tissue revealed two layers of mature osteoblasts and just a few cells in the collagenous space between the apical and basal layers (Figure 4F). This recapitulates the physiological environment, in that, during bone formation, osteoblasts line the new bone's surface after laying down a collagenous matrix.[4] Moreover, TEM images show distinctive banded patterns for fibrils due to the overlapping pattern of the tropocollagen units. Utilizing the coated microdevice, metastatic breast cancer cells MDA-MB-231 and the non-metastatic variant, MDA-MB-231-BMRS1 were then used to examine and compare metastatic niche formation in the osteoblastic tissue. After two weeks, MDA-MB-231-BMRS1 cells did not form any large colonies and did not invade into the matrix; moreover, the cells were loosely attached to the apical surface of the osteoblastic tissue. However, MDA-MB-231 cells caused erosion of the apical collagen in the first week and created large holes and protruded long invadopodia in the second week. Additionally, in the second week, osteoblastic tissue started to reorganize to a more elongated morphology, and cancer cells started proliferating into strings of cells aligned with the elongated axis of the collagenous matrix, which is similar to the clinical observation of cancer cells.[155]

Cell-laden hydrogels are currently unable to replicate the complexity of highly mineralized bone tissue, and mineral deposition is limited to small and dispersed mineral nodules appearing after 14–21 days of culture. However, in the microfluidic community, the addition of hydroxyapatite (HA) nanoparticles to the ECM has been applied to resemble mineralized bone tissue.[156, 157] It should be noted that HA nanoparticles inhibit proliferation and induce apoptosis by producing intracellular reactive oxygen species (ROS) and activating p53, resulting in DNA damage.[158] For example, Ahn *et al.* used a three-gel channel to investigate the interactions between the tumor and bone mimicking microenvironment (Figure 4G).[156] In this study, they used fibroblasts instead of osteoblasts due to their genetic similarities within the bone matrix.[159] To study cancer migration through the HA/fibrin gel, the central gel channel and one of the side gel channels were filled with 2.5 mg/ml HA/fibrin gel and fibrin gel, respectively, while the other side-channel was filled with fibrin gel embedded with fibroblasts (4H). Initial results published by Jusoh *et al.* showed that adding more than 0.5% HA would make the gel not polymerize.[157] After adding human colon cancer (SW620) and human gastric cancer (MKN74) cells, the results showed a decrease in extravasated cells by increasing HA concentrations. Moreover, to evaluate microenvironment induced angiogenesis, cancer cells were co-cultured with fibroblasts within the HA/fibrin matrix, and then endothelial cells were introduced to form a monolayer on the media channel (Figure 4I). The results showed that as the HA concentration increased, the sprout lengths decreased because HA induced secretion of factors that suppressed angiogenesis. Finally, to mimic the crosstalk between the tumor and the microenvironment, microspheroids of tumor-fibroblast were cultured in HA/fibrin matrix in the gel channel with the endothelial cells patterned on the side channel (Figure 4J). Angiogenesis induced by SW620-fibroblast microspheroids caused thinner blood vessels compared to MKN74-fibroblast spheroids.

Author Manuscript Author Manuscript Author Manuscript Author Manuscript

After the arrest of cancer cells in capillaries, biochemical factors secreted by all the cells in the microenvironment will guide them to extravasate out of the vessel.[160] Bersini *et al.* investigated the signaling pathway involving the osteoblast-secreted inflammatory chemokine CXCL5 and the breast cancer cell surface receptor CXCR2 using the bone on a chip microfluidic device.[161] CXCL5 is known to activate Snail, a transcription factor involved in cancer cell invasiveness and migration. Moreover, it has been demonstrated that Snail overexpression in breast cancer cells can upregulate Axl expression, a tyrosine kinase receptor, which, in turn, is important for extravasation.[162–164] Incubation of cancer cells with CXCR2 blocking antibody decreased the extravasation percentage in the OD hBM-MSCs embedded collagen gel (77.5 ± 3.7% vs. 45.8 ± 5.4%) while it had no significant effect on the distance traveled by extravasated cells (46 ± 5.7 vs. 50.8 ± 6.2 μm) (Figure 5A, 5B, and 5E). This suggests that CXCR2 only plays a minor role in cancer cell migration within a bone-mimicking environment. However, the addition of CXCL5 ligand to collagen gel increased the extravasation rate (37.6 ± 7.3% vs. 78.3 ± 9.7%) as well as the migrated distance (31.8 ± 5.0 vs. 54.7 ± 5.8 μm), as compared to the control (Figure 5C, 5D, and 5E). In another bone-on-chip system with engineered microcapillaries, the researchers introduced a katushka-expressing bone-seeking clone (BOKL) of the MDA-MB-231 metastatic breast cancer cell line to investigate extravasation into gel embedded with OD hBM-MSCs, to mimic the bone environment or the gel embedding C2C12 myoblasts, as a muscle mimicking environment (Figure 5F).[106] The cancer cell extravasation rate was remarkably higher in the bone mimicking environment (56.5 ± 4.8%) compared to muscle mimicking environment (8.2 ± 2.3%) or without stromal cell addition (14.7 ± 3.6%). This large difference was not observed in the previous studies due to the less physiological environment tested before. The permeability values of the microvasculature were measured, and interestingly the muscle-mimicking environment, as the leakiest ($8.37 \times 10^{-6} \pm 1.53 \times 10^{-6}$ cm/s, a 2.0-fold increase compared to bone mimicking environment), caused the lowest extravasation rate. In the same study, the effect of the A3 adenosine receptor (A3AR) expressed by many cancer cell types as an antimetastatic factor was studied. A3AR antagonist PBS-10 within C2C12 containing microfluidic device was introduced, and cancer cells were pre-incubated with A3AR before seeding. The results show a significant decrease and increase in the extravasation rate (12.7 ± 2.8% compared to 56.5 ± 4.8%) (Figure 5G) and microvessel permeability ($8.22 \times 10^{-6} \pm 1.76 \times 10^{-6}$ cm/s compared with $4.12 \times 10^{-6} \pm 0.75 \times 10^{-6}$ cm/s) (Figure 5H). Moreover, they studied the effects of flow rate (2 μl/min) in the medium channel on microvasculature architecture and extravasation rate and distance. In the presence of the flow, endothelial cells have an elongated morphology and actin filaments aligned with the flow direction, which resembles the *in-vivo* microvessels. The flow caused a 2.4-fold decrease in microvessel permeability and a significantly lower extravasation rate. However, the extravasation distance in the case of flow was increased.

Bone marrow is the soft and highly vascular tissue located within the cancellous portion of the bone, which contains hematopoietic stem cells, marrow adipose tissue, and supportive stromal cells.[165] Particularly, the endosteal niche of the bone marrow has been increasingly associated with normal marrow function and leukemias.[166] Hematopoietic stem cells (HSCs) are a rare subpopulation of hematopoietic cells residing in bone marrow with the ability to give rise to blood cells, including leukocytes, erythrocytes, and thrombocytes.

Author Manuscript Author Manuscript Author Manuscript Author Manuscript

[167, 168] The *in-vitro* microfluidic models of human hematopoiesis have helped researchers to better understand bone marrow physiology through culturing stem and progenitor cells surrounded by stromal cells as well as endothelium-lined vasculature.[169–173] Initially, Torsisawa *et al.* introduced a method that involved engineering new bone *in-vivo*, which was then removed and cultured in a microfluidic device.[170] This bone marrow model was tested as an *in-vitro* radiation toxicity platform, and it was shown that a statistically significant decrease in the proportions of HSCs, hematopoietic progenitors, lymphoid cells, and myeloid cells similar to *in-vivo* irradiated mice was observed. In recent years, several studies have been conducted to recreate the *in-vitro* bone marrow on-chip without using animals. For example, Aleman *et al.* developed a microfluidic chip with a recirculating perfusion system, which included biomimicry parameters such as 3D architecture and cell-cell / cell-matrix interactions.[173] Recently, the Ingber group introduced a novel microfluidic device containing CD34+ cells and bone marrow-derived stromal cells (BMSCs) with an endothelium-lined vascular channel that can recapitulate myeloerythroid toxicity after exposure to chemotherapeutic drugs and radiation as well as its recovery after introducing drugs.[174] It should be noted that due to the key role of bone marrow in immune systems with hematopoietic activities, it is important to develop bone marrow on-chip models that support immunogenicity and immunotoxicity testing. Overall, the human bone marrow on-chip systems can be used to recapitulate many clinical characteristics of bone marrow physiology and its response to various stimuli.

6. Limitations and future directions

Although microfluidic devices enable the investigation of a myriad of cell-cell and cell-matrix interactions under conditions that are specific to the bone microenvironment and relevant for various diseases, several challenges still exist. For instance, it has been extensively shown that mechanical loading is an imperative component of bone tissue function and physiology.[175–178] Osteocyte biology in the native tissue is highly responsive to mechanical effects, and the types of loads distributed across osteon units[6, 179] are difficult to recapitulate with pure flow shear stresses. Microdevices that incorporate controllable and cyclic mechanical stresses have been widely developed in the field. However, bone-on-a-chip systems that combine complex loading and heterotypic tissue designs (with vascular capillaries, multiple cell types, and tissue components) have remained elusive. These are likely to represent the next set of organ-on-a-chip model systems that truly replicate the complexity of bone tissue dynamics.

Additionally, despite extensive work, current strategies to mimic bone tissue on-a-chip fall short in approximating the real complexity of the cellularized and calcified bone microenvironment. Bone tissue is inherently a cell-loaded biomaterial where cells are cemented within a nanoscale calcified matrix composed of a non-mineralized organic component (predominantly collagen I) and a mineralized inorganic component along with over 200 different types of noncollagenous proteins (NCPs).[3, 180] The conventional model systems used to study bone function and cell response to bone-like microenvironments are usually based on pre-calcified polymer or bioceramics. Calcium phosphate (CaP) ceramics such as synthetic hydroxyapatite (HA) [$Ca_{10}(PO_4)_6(OH)_2$], beta tricalcium phosphate (βTCP) [$Ca_3(PO4)_2$], have been widely used since they not only resemble the native bone

Author Manuscript Author Manuscript Author Manuscript Author Manuscript

chemical composition but also they can enhance cellular activity and bone repair.[181] In particular, HA, which has enhanced osteoinductivity, has relative high stability, which decreases its degradation and slows down the native process of tissue remodeling, since, in native bone, the nanostructure of the HA crystallites together with the organic matrix and cells will invariably contribute to tissue degradation, which does not happen in pure HA biomaterials. On the other hand, βTCP can degrade 10–20 times faster than HA, and thus it may provide the Ca and P ions needed for enhanced cellular functions.[182] However, these models usually fail to replicate the complexity of bone cellular or micro and nanoscale ECM structural environment. Moreover, incorporating these rigid substrates within microfluidic devices is challenging.

On the other hand, cell-laden hydrogels have been considered as an alternative approach to recreating 3D cellular and structural environment. Several hydrogel biomaterials, including natural polymers (such as collagen, fibrin, gelatin, hyaluronic acid, chitosan, and alginate) and synthetic polymers (such as poly(ethylene glycol) (PEG), poly(ethylene oxide) (PEO), poly(vinyl alcohol) (PVA), poly (acrylic acid) (PAA), and poly(propylene fumarate-co-ethylene glycol) (P(PF-co-EG)), among many others) have been used as biomaterials for bone-related studies.[183] Importantly, in the field of bone microfluidics, collagen and fibrin have been the most commonly used biomaterials, likely because they enable cell encapsulation and approximate key aspects of the bone ECM while being easily integrated into microfluidic devices. As the basic element of the most connective tissues and the most abundant protein in mammalian tissues, collagen has been widely used for bone tissue engineering purposes. Collagen type I is the primary component of the bone matrix, and it consists of three polypeptide chains helically coiled around to form microfibrillar structures.[184] The other highly used biomaterial, fibrin, is formed by the action of thrombin on fibrinogen in the final step of the clotting cascade.[185] Fibrin can bind to numerous proteins (such as fibronectin and vitronectin) and growth factors (such as FGF, VEGF, and IGF-1).[186] Additionally, its unique viscoelastic behavior can increase its stiffness up to 20-fold at large strains, which has been found beneficial in long-term microfluidic experiments.[185] Furthermore, it has been shown that mixtures of type I collagen and fibrin gels could promote vascular formation without gel retraction, in various integrin-dependent mechanisms.[187]

Despite the widespread use of cell-laden hydrogel in bone microfluidic studies, current methods that rely on cell-laden hydrogels are either not mineralized or simply combined with calcium and phosphate micro/nanoparticles. Therefore, perhaps the most critical component of the bone matrix is overlooked in these said strategies. Similarly, methods to stimulate calcium deposition by osteoprogenitor cells within these cell-laden biomaterials remain dependent upon the use of exogenous supplements (beta glycerol phosphate, ascorbic acid, and dexamethasone), which are not natural components of bone tissue, and are known to induce slow, dispersed and poorly coordinated secretion mineral nodules across the matrix, which do not mimic the coordinated and rapidly moving mineralization front found in bone tissue. We have recently addressed these limitations by developing cell-laden hydrogels that are controllably mineralized at the nanoscale to match the nanostructure, chemical composition, and mechanical properties of native bone with the ability to support vasculature and innervation (Figure 6).[188] These engineered tissues have shown a unique

Author Manuscript Author Manuscript Author Manuscript Author Manuscript

trophic effect on prostate cancer *in-vivo* and have been proposed as a useful model system to study cancer-bone interactions *in-vitro*. Current studies in our lab have successfully attempted to miniaturize this process to enable calcification of vascularized and bone cell-laden matrix materials on-chip (Figure 6M). These biomimetic strategies should offer another layer of development towards approximating the true complexity of bone tissue as a controllably engineered biomaterial. These nanoscale mineralized materials are thought to be especially relevant for cancer studies since it has been demonstrated that the orientation and crystallinity of nanoscale HA mineral is a crucial determinant in the homing of metastatic cancers to specific sites in the bone matrix.[189] Therefore, miniaturizing these bone-like microenvironments on-a-chip is likely to open up new opportunities for an improved understanding of the interactions between bone tissue and cancer cells.

Furthermore, recent developments in liquid-phase and cryogenic TEM have enabled unprecedented visualization of dynamic biomineralization phenomena with sub-nanometer resolution.[190] Although the far majority of these bone-related materials phenomena have been studied away from the context of cell biology, recent efforts form expert groups have been focused on combining organ-on-a-chip technologies with high-resolution microscopy to elucidate the sub-nanometer events that take place during biological regulation of bone biomineralization. The possible outcomes resulting from these studies are likely to break new ground in the understanding of bone biology and should provide an important bridge between the fields of high-resolution microscopy, tissue engineering, and cell biology.

Moreover, recent examples illustrating the possibilities for integrating multiple organs on microfluidic breadboards,[191, 192] inclusive of multi-organ systems showing metastatic processes from one organ-chip to another, is an area that should be further investigated in bone microfluidics. The possibility of replicating and testing the long-held seed and soil hypothesis of cancer metastasis to bone in multi-organ chips is a unique opportunity. Future studies should address these goals. Lastly, the use of bone on-a-chip microdevices as tools for point-of-care precision medicine is the area that should bring bone microfluidics closer to clinical medicine. The ability to isolate patient cells from the bed-side, seeding them in high-throughput microfluidic devices, and testing specific drugs and drug combinations, will potentially open up a new era in modern bone therapeutics. The technologies for such end goals are largely available. However, much more comprehensive integration of clinicians, industry, and academic research will be necessary to enable these goals.

Supplementary Material

Refer to Web version on PubMed Central for supplementary material.

Acknowledgments

This project was partly supported by funding from the National Institute of Dental and Craniofacial Research (R01DE026170), OHSU-UO, and OHSU-PSU Collaborative Seed Projects.

Author Manuscript Author Manuscript Author Manuscript Author Manuscript

Biographies

Amin Mansoorifar obtained his Ph.D. in Mechanical Engineering at Southern Methodist University, Dallas in 2019. He received his B.Sc. and M.Sc. degrees in Mechanical Engineering from Shiraz University, Iran in 2012 and 2014, respectively. He joined Bertassoni lab at Oregon Health and Science University as a postdoctoral scholar on August 2019. His primary research interests are Micro, Nano, and Biofluidics with a specific focus on the development of new microfluidic platforms for biological studies.

Luiz E. Bertassoni received his dental degree from Brazil, PhD in Biomaterials from University of Sydney, and had been a postdoctoral scholar at University of California San Francisco, and the Harvard-MIT Division of Health Sciences and Technology. He is currently an Associate Professor at Oregon Health and Science University, where he holds appointments in School of Dentistry, Department of Biomedical Engineering, Cancer Early Detection Advanced Research Center (CEDAR), and OHSU Center for Regenerative Medicine. His research is focused on micro-scale technologies and bioprinting for tissue regeneration, nanoscale structural and mechanical properties of mineralized tissues, and organs-on-a-chip.

References

1. Datta H, et al. , The cell biology of bone metabolism. Journal of clinical pathology, 2008. 61(5): p. 577–587. [PubMed: 18441154]
2. Robling AG, Castillo AB, and Turner CH, Biomechanical and molecular regulation of bone remodeling. Annu. Rev. Biomed. Eng, 2006. 8: p. 455–498. [PubMed: 16834564]
3. Florencio-Silva R, et al. , Biology of bone tissue: structure, function, and factors that influence bone cells. BioMed research international, 2015. 2015.
4. Clarke B, Normal bone anatomy and physiology. Clinical journal of the American Society of Nephrology, 2008. 3(Supplement 3): p. S131–S139. [PubMed: 18988698]
5. Teitelbaum SL, Osteoclasts: what do they do and how do they do it? The American journal of pathology, 2007. 170(2): p. 427–435. [PubMed: 17255310]
6. Bonewald LF, The amazing osteocyte. Journal of bone and mineral research, 2011. 26(2): p. 229–238. [PubMed: 21254230]
7. General Oo.t.S., The Basics of Bone in Health and Disease, in Bone Health and Osteoporosis: A Report of the Surgeon General. 2004, Office of the Surgeon General (US).
8. Feng X. and McDonald JM, Disorders of bone remodeling. Annual review of pathology, 2011. 6: p. 121–145.

Author Manuscript Author Manuscript Author Manuscript Author Manuscript

9. Dempster DW, Osteoporosis and the burden of osteoporosis-related fractures. American Journal of Managed Care, 2011. 17(6): p. S164.
10. Roche J, et al. , Effect of comorbidities and postoperative complications on mortality after hip fracture in elderly people: prospective observational cohort study. Bmj, 2005. 331(7529): p. 1374. [PubMed: 16299013]
11. Macedo F, et al. , Bone Metastases: An Overview. Oncology reviews, 2017. 11(1): p. 321–321. [PubMed: 28584570]
12. Wittkowske C, et al. , In Vitro Bone Cell Models: Impact of Fluid Shear Stress on Bone Formation. Frontiers in Bioengineering and Biotechnology, 2016. 4(87).
13. Pearce A, et al. , Animal models for implant biomaterial research in bone: a review. Eur Cell Mater, 2007. 13(1): p. 1–10. [PubMed: 17334975]
14. Xu L, et al. , Precision therapeutic targeting of human cancer cell motility. Nature Communications, 2018. 9(1): p. 2454.
15. Zhang L, et al. , A multi-functional therapy approach for cancer: targeting Raf1- mediated inhibition of cell motility, growth and interaction with the microenvironment. Mol Cancer Ther, 2020.
16. Katt ME, et al. , In vitro tumor models: advantages, disadvantages, variables, and selecting the right platform. Frontiers in bioengineering and biotechnology, 2016. 4: p. 12. [PubMed: 26904541]
17. Portillo-Lara R. and Annabi N, Microengineered cancer-on-a-chip platforms to study the metastatic microenvironment. Lab on a chip, 2016. 16(21): p. 4063–4081. [PubMed: 27605305]
18. McGonigle P. and Ruggeri B, Animal models of human disease: challenges in enabling translation. Biochem Pharmacol, 2014. 87(1): p. 162–71. [PubMed: 23954708]
19. Ruggeri BA, Camp F, and Miknyoczki S, Animal models of disease: pre-clinical animal models of cancer and their applications and utility in drug discovery. Biochem Pharmacol, 2014. 87(1): p. 150–61. [PubMed: 23817077]
20. Cekanova M. and Rathore K, Animal models and therapeutic molecular targets of cancer: utility and limitations. Drug design, development and therapy, 2014. 8: p. 1911–1921.
21. Chen Z, Zilberberg J, and Lee W, Pumpless microfluidic device with open top cell culture under oscillatory shear stress. Biomedical Microdevices, 2020. 22(3): p. 1–10.
22. Chen Z, et al. , Pumpless platform for high-throughput dynamic multicellular culture and chemosensitivity evaluation. Lab on a Chip, 2019. 19(2): p. 254–261. [PubMed: 30547180]
23. Choudhary S, et al. , Hypoxic three-dimensional cellular network construction replicates ex vivo the phenotype of primary human osteocytes. Tissue Engineering Part A, 2018. 24(5–6): p. 458–468. [PubMed: 28594289]
24. Halldorsson S, et al. , Advantages and challenges of microfluidic cell culture in polydimethylsiloxane devices. Biosensors and Bioelectronics, 2015. 63: p. 218–231. [PubMed: 25105943]
25. Jiang W, et al. , Cell-laden microfluidic microgels for tissue regeneration. Lab on a Chip, 2016. 16(23): p. 4482–4506. [PubMed: 27797383]
26. Bettinger CJ and Borenstein JT, Biomaterials-based microfluidics for engineered tissue constructs. Soft Matter, 2010. 6(20): p. 4999–5015.
27. Whitesides GM, The origins and the future of microfluidics. Nature, 2006. 442(7101): p. 368–373. [PubMed: 16871203]
28. Holmes D. and Gawad S, The application of microfluidics in biology, in Microengineering in biotechnology. 2010, Springer. p. 55–80.
29. Weibel DB and Whitesides GM, Applications of microfluidics in chemical biology. Current opinion in chemical biology, 2006. 10(6): p. 584–591. [PubMed: 17056296]
30. Breslauer DN, Lee PJ, and Lee LP, Microfluidics-based systems biology. Molecular Biosystems, 2006. 2(2): p. 97–112. [PubMed: 16880927]
31. Mitchell P, Microfluidics—downsizing large-scale biology. Nature biotechnology, 2001. 19(8): p. 717–721.

Author Manuscript Author Manuscript Author Manuscript Author Manuscript

32. Bhise NS, et al. , Organ-on-a-chip platforms for studying drug delivery systems. Journal of Controlled Release, 2014. 190: p. 82–93. [PubMed: 24818770]
33. Zhang B. and Radisic M, Organ-on-a-chip devices advance to market. Lab on a Chip, 2017. 17(14): p. 2395–2420. [PubMed: 28617487]
34. Ahadian S, et al. , Organ-on-a-chip platforms: a convergence of advanced materials, cells, and microscale technologies. Advanced healthcare materials, 2018. 7(2): p. 1700506.
35. Caplin JD, et al. , Microfluidic organ-on-a-chip technology for advancement of drug development and toxicology. Advanced healthcare materials, 2015. 4(10): p. 1426–1450. [PubMed: 25820344]
36. Lee JB and Sung JH, Organ-on-a-chip technology and microfluidic whole-body models for pharmacokinetic drug toxicity screening. Biotechnology journal, 2013. 8(11): p. 1258–1266. [PubMed: 24038956]
37. Kimura H, Sakai Y, and Fujii T, Organ/body-on-a-chip based on microfluidic technology for drug discovery. Drug metabolism and pharmacokinetics, 2018. 33(1): p. 43–48. [PubMed: 29175062]
38. Selimović Š, Dokmeci MR, and Khademhosseini A, Organs-on-a-chip for drug discovery. Current opinion in pharmacology, 2013. 13(5): p. 829–833. [PubMed: 23850526]
39. Huh D, A human breathing lung-on-a-chip. Annals of the American Thoracic Society, 2015. 12(Supplement 1): p. S42–S44. [PubMed: 25830834]
40. Stucki AO, et al. , A lung-on-a-chip array with an integrated bio-inspired respiration mechanism. Lab on a Chip, 2015. 15(5): p. 1302–1310. [PubMed: 25521475]
41. Wilmer MJ, et al. , Kidney-on-a-chip technology for drug-induced nephrotoxicity screening. Trends in biotechnology, 2016. 34(2): p. 156–170. [PubMed: 26708346]
42. Nieskens TT and Wilmer MJ, Kidney-on-a-chip technology for renal proximal tubule tissue reconstruction. European journal of pharmacology, 2016. 790: p. 46–56. [PubMed: 27401035]
43. Agarwal A, et al. , Microfluidic heart on a chip for higher throughput pharmacological studies. Lab on a Chip, 2013. 13(18): p. 3599–3608. [PubMed: 23807141]
44. Marsano A, et al. , Beating heart on a chip: a novel microfluidic platform to generate functional 3D cardiac microtissues. Lab on a Chip, 2016. 16(3): p. 599–610. [PubMed: 26758922]
45. Pocock K, et al. , Intestine-on-a-chip microfluidic model for efficient in vitro screening of oral chemotherapeutic uptake. ACS Biomaterials Science & Engineering, 2017. 3(6): p. 951–959. [PubMed: 33429567]
46. Jalili-Firoozinezhad S, et al. , A complex human gut microbiome cultured in an anaerobic intestine-on-a-chip. Nature biomedical engineering, 2019. 3(7): p. 520.
47. França CM, et al. , The tooth on-a-chip: a microphysiologic model system mimicking the biologic interface of the tooth with biomaterials. Lab on a Chip, 2020.
48. Zheng F, et al. , Organ-on-a-Chip Systems: microengineering to biomimic living systems. Small, 2016. 12(17): p. 2253–2282. [PubMed: 26901595]
49. Doryab A, Amoabediny G, and Salehi-Najafabadi A, Advances in pulmonary therapy and drug development: Lung tissue engineering to lung-on-a-chip. Biotechnology advances, 2016. 34(5): p. 588–596. [PubMed: 26875777]
50. Zhang YS, et al. , From cardiac tissue engineering to heart-on-a-chip: beating challenges. Biomedical Materials, 2015. 10(3): p. 034006.
51. Bein A, et al. , Microfluidic organ-on-a-chip models of human intestine. Cellular and molecular gastroenterology and hepatology, 2018. 5(4): p. 659–668. [PubMed: 29713674]
52. Garg P, et al. , Prospective review of mesenchymal stem cells differentiation into osteoblasts. Orthopaedic surgery, 2017. 9(1): p. 13–19. [PubMed: 28276640]
53. Rosenberg N, Rosenberg O, and Soudry M, Osteoblasts in bone physiology—mini review. Rambam Maimonides medical journal, 2012. 3(2).
54. Heino TJ and Hentunen TA, Differentiation of osteoblasts and osteocytes from mesenchymal stem cells. Current stem cell research & therapy, 2008. 3(2): p. 131–145. [PubMed: 18473879]
55. Franz-Odendaal TA, Hall BK, and Witten PE, Buried alive: how osteoblasts become osteocytes. Developmental dynamics: an official publication of the American Association of Anatomists, 2006. 235(1): p. 176–190. [PubMed: 16258960]

Author Manuscript Author Manuscript Author Manuscript Author Manuscript

56. Aarden EM, Nijweide PJ, and Burger EH, Function of osteocytes in bone. Journal of cellular biochemistry, 1994. 55(3): p. 287–299. [PubMed: 7962159]
57. Bilezikian JP, Raisz LG, and Martin TJ, Principles of bone biology. 2008: Academic press.
58. Rutkovskiy A, Stensløkken K-O, and Vaage IJ, Osteoblast Differentiation at a Glance. Medical science monitor basic research, 2016. 22: p. 95–106. [PubMed: 27667570]
59. Michael Delaine-Smith R, et al. , Preclinical models for in vitro mechanical loading of bone-derived cells. BoneKEy reports, 2015. 4: p. 728–728. [PubMed: 26331007]
60. Mullender M, et al. , Mechanotransduction of bone cells in vitro: mechanobiology of bone tissue. Med Biol Eng Comput, 2004. 42(1): p. 14–21. [PubMed: 14977218]
61. Altman GH, et al. , Cell differentiation by mechanical stress. The FASEB Journal, 2002. 16(2): p. 1–13. [PubMed: 11772930]
62. Thompson WR, Rubin CT, and Rubin J, Mechanical regulation of signaling pathways in bone. Gene, 2012. 503(2): p. 179–193. [PubMed: 22575727]
63. Velve-Casquillas G, et al. , Microfluidic tools for cell biological research. Nano today, 2010. 5(1): p. 28–47. [PubMed: 21152269]
64. Babaliari E, Petekidis G, and Chatzinikolaidou M, A precisely flow-controlled microfluidic system for enhanced pre-osteoblastic cell response for bone tissue engineering. Bioengineering, 2018. 5(3): p. 66.
65. Schaffler MB, et al. , Osteocytes: master orchestrators of bone. Calcified tissue international, 2014. 94(1): p. 5–24. [PubMed: 24042263]
66. Dallas SL, Prideaux M, and Bonewald LF, The osteocyte: an endocrine cell … and more. Endocrine reviews, 2013. 34(5): p. 658–690. [PubMed: 23612223]
67. Riquelme MA, et al. , The Role of Connexin Channels in the Response of Mechanical Loading and Unloading of Bone. International journal of molecular sciences, 2020. 21(3): p. 1146.
68. Matsuo K, Cross-talk among bone cells. Curr Opin Nephrol Hypertens, 2009. 18(4): p. 292–7. [PubMed: 19395964]
69. Marie P, Bone remodeling: a social network of cells. Medicographia, 2012. 34(2): p. 149–155.
70. Zhang J-N, et al. , The role of the sphingosine-1-phosphate signaling pathway in osteocyte mechanotransduction. Bone, 2015. 79: p. 71–78. [PubMed: 25988659]
71. Jacobs C, et al. , Differential effect of steady versus oscillating flow on bone cells. Journal of biomechanics, 1998. 31(11): p. 969–976. [PubMed: 9880053]
72. Middleton K, et al. , Microfluidic co-culture platform for investigating osteocyte-osteoclast signalling during fluid shear stress mechanostimulation. Journal of biomechanics, 2017. 59: p. 35–42. [PubMed: 28552413]
73. Kohli SS and Kohli VS, Role of RANKL-RANK/osteoprotegerin molecular complex in bone remodeling and its immunopathologic implications. Indian journal of endocrinology and metabolism, 2011. 15(3): p. 175–181. [PubMed: 21897893]
74. Luo G, et al. , TNF-α and RANKL promote osteoclastogenesis by upregulating RANK via the NF-κB pathway. Molecular medicine reports, 2018. 17(5): p. 6605–6611. [PubMed: 29512766]
75. Han Y, et al. , Paracrine and endocrine actions of bone—the functions of secretory proteins from osteoblasts, osteocytes, and osteoclasts. Bone Research, 2018. 6(1): p. 16. [PubMed: 29844945]
76. Yan Y, et al. , Osteocyte-Mediated Translation of Mechanical Stimuli to Cellular Signaling and Its Role in Bone and Non-bone-Related Clinical Complications. Current Osteoporosis Reports, 2020. 18(1): p. 67–80. [PubMed: 31953640]
77. Meshcheryakova A, Mechtcheriakova D, and Pietschmann P, Sphingosine 1-phosphate signaling in bone remodeling: multifaceted roles and therapeutic potential. Expert opinion on therapeutic targets, 2017. 21(7): p. 725–737. [PubMed: 28524744]
78. Amini AR, Laurencin CT, and Nukavarapu SP, Bone tissue engineering: recent advances and challenges. Critical reviews in biomedical engineering, 2012. 40(5): p. 363–408. [PubMed: 23339648]
79. Lin Z, et al. , Osteochondral Tissue Chip Derived From iPSCs: Modeling OA Pathologies and Testing Drugs. Frontiers in Bioengineering and Biotechnology, 2019. 7(411).

Author Manuscript Author Manuscript Author Manuscript Author Manuscript

80. De Riccardis G, et al. A 3D printed microfluidic bioreactor to engineering biphasic construct. in TISSUE ENGINEERING PART A. 2017. MARY ANN LIEBERT, INC 140 HUGUENOT STREET, 3RD FL, NEW ROCHELLE, NY 10801 USA.
81. Lin H, et al. , Stem cell-based microphysiological osteochondral system to model tissue response to interleukin-1β. Mol Pharm, 2014. 11(7): p. 2203–12. [PubMed: 24830762]
82. Lee J-H, et al. , Microfluidic 3D bone tissue model for high-throughput evaluation of wound-healing and infection-preventing biomaterials. Biomaterials, 2012. 33(4): p. 999–1006. [PubMed: 22061488]
83. Doyle AD, et al. , Dimensions in cell migration. Current Opinion in Cell Biology, 2013. 25(5): p. 642–649. [PubMed: 23850350]
84. Moreno-Arotzena O, et al. , Inducing chemotactic and haptotactic cues in microfluidic devices for three-dimensional in vitro assays. Biomicrofluidics, 2014. 8(6): p. 064122.
85. Moreno-Arotzena O, et al. , Fibroblast Migration in 3D is Controlled by Haptotaxis in a Non-muscle Myosin II-Dependent Manner. Annals of Biomedical Engineering, 2015. 43(12): p. 3025–3039. [PubMed: 26014363]
86. Movilla N, et al. , Degradation of extracellular matrix regulates osteoblast migration: A microfluidic-based study. Bone, 2018. 107: p. 10–17. [PubMed: 29107125]
87. Bartok B. and Firestein GS, Fibroblast-like synoviocytes: key effector cells in rheumatoid arthritis. Immunological reviews, 2010. 233(1): p. 233–255. [PubMed: 20193003]
88. Bottini N. and Firestein GS, Duality of fibroblast-like synoviocytes in RA: passive responders and imprinted aggressors. Nature reviews. Rheumatology, 2013. 9(1): p. 24–33. [PubMed: 23147896]
89. Bustamante MF, et al. , Fibroblast-like synoviocyte metabolism in the pathogenesis of rheumatoid arthritis. Arthritis Research & Therapy, 2017. 19(1): p. 110. [PubMed: 28569176]
90. Ma H-P, et al. , A microfluidic chip-based co-culture of fibroblast-like synoviocytes with osteoblasts and osteoclasts to test bone erosion and drug evaluation. Royal Society open science, 2018. 5(9): p. 180528.
91. Li G. q., et al. , Anti-invasive effects of celastrol in hypoxia-induced fibroblast-like synoviocyte through suppressing of HIF-1α/CXCR4 signaling pathway. International immunopharmacology, 2013. 17(4): p. 1028–1036. [PubMed: 24144813]
92. Li G, et al. , Celastrol inhibits lipopolysaccharide-stimulated rheumatoid fibroblast-like synoviocyte invasion through suppression of TLR4/NF-κB-mediated matrix metalloproteinase-9 expression. PloS one, 2013. 8(7).
93. Filipowska J, et al. , The role of vasculature in bone development, regeneration and proper systemic functioning. Angiogenesis, 2017. 20(3): p. 291–302. [PubMed: 28194536]
94. Tomlinson RE and Silva MJ, Skeletal Blood Flow in Bone Repair and Maintenance. Bone Res, 2013. 1(4): p. 311–22. [PubMed: 26273509]
95. Brandi ML and Collin-Osdoby P, Vascular biology and the skeleton. J Bone Miner Res, 2006. 21(2): p. 183–92. [PubMed: 16418774]
96. Mannino RG, Qiu Y, and Lam WA, Endothelial cell culture in microfluidic devices for investigating microvascular processes. Biomicrofluidics, 2018. 12(4): p. 042203.
97. Khan OF and Sefton MV, Endothelial cell behaviour within a microfluidic mimic of the flow channels of a modular tissue engineered construct. Biomed Microdevices, 2011. 13(1): p. 69–87. [PubMed: 20842530]
98. Bertassoni LE, et al. , Hydrogel bioprinted microchannel networks for vascularization of tissue engineering constructs. Lab on a Chip, 2014. 14(13): p. 2202–2211. [PubMed: 24860845]
99. Kuzmic N, et al. , Modelling of endothelial cell migration and angiogenesis in microfluidic cell culture systems. Biomech Model Mechanobiol, 2019. 18(3): p. 717–731. [PubMed: 30604299]
100. Guo Z, et al. , Validation of a Vasculogenesis Microfluidic Model for Radiobiological Studies of the Human Microvasculature. Advanced Materials Technologies, 2019. 4(4): p. 1800726.
101. Costa L, et al., Microfluidics for Angiogenesis Research, in Biomaterials-and Microfluidics-Based Tissue Engineered 3D Models. 2020, Springer. p. 97–119.
102. Ahn J, et al. , Pneumatically Actuated Microfluidic Platform for Reconstituting 3D Vascular Tissue Compression. Applied Sciences, 2020. 10(6): p. 2027.

Author Manuscript Author Manuscript Author Manuscript Author Manuscript

103. Song H-HG, et al. , Transient Support from Fibroblasts is Sufficient to Drive Functional Vascularization in Engineered Tissues. Advanced Functional Materials. n/a(n/a): p. 2003777.
104. Takehara H, et al. , Microfluidic vascular-bed devices for vascularized 3D tissue engineering: tissue engineering on a chip. Biomedical Microdevices, 2019. 22(1): p. 9. [PubMed: 31863202]
105. Fleischer S, Tavakol DN, and Vunjak-Novakovic G, From Arteries to Capillaries: Approaches to Engineering Human Vasculature. Advanced Functional Materials, 2020. 30(37): p. 1910811.
106. Jeon JS, et al. , Human 3D vascularized organotypic microfluidic assays to study breast cancer cell extravasation. Proceedings of the National Academy of Sciences, 2015. 112(1): p. 214–219.
107. Pagella P. and Mitsiadis TA, Analysis of Tooth Innervation in Microfluidic Coculture Devices, in Stem Cells and Tissue Repair. 2020, Springer. p. 99–106.
108. Vysokov N, McMahon SB, and Raouf R, The role of Na V channels in synaptic transmission after axotomy in a microfluidic culture platform. Scientific reports, 2019. 9(1): p. 1–13. [PubMed: 30626917]
109. Leitão L, et al. , Osteoblasts are inherently programmed to repel sensory innervation. Bone Research, 2020. 8(1): p. 20. [PubMed: 32435517]
110. Chenu C, Role of innervation in the control of bone remodeling. Journal of Musculoskeletal and Neuronal Interactions, 2004. 4(2): p. 132. [PubMed: 15615111]
111. Serre C, et al. , Evidence for a dense and intimate innervation of the bone tissue, including glutamate-containing fibers. Bone, 1999. 25(6): p. 623–629. [PubMed: 10593406]
112. Silva DI, et al. , Dorsal root ganglion neurons regulate the transcriptional and translational programs of osteoblast differentiation in a microfluidic platform. Cell death & disease, 2017. 8(12): p. 1–14. [PubMed: 29233966]
113. Klein CA, The metastasis cascade. Science, 2008. 321(5897): p. 1785–1787. [PubMed: 18818347]
114. Seyfried TN and Huysentruyt LC, On the origin of cancer metastasis. Critical reviews in oncogenesis, 2013. 18(1–2): p. 43. [PubMed: 23237552]
115. Gómez-Cuadrado L, et al. , Mouse models of metastasis: progress and prospects. Disease models & mechanisms, 2017. 10(9): p. 1061–1074. [PubMed: 28883015]
116. Park SI, et al. , Preclinical mouse models of human prostate cancer and their utility in drug discovery. Current protocols in pharmacology, 2010. 51(1): p. 14.15. 1–14.15. 27.
117. Sanmamed MF, et al. , Defining the optimal murine models to investigate immune checkpoint blockers and their combination with other immunotherapies. Ann Oncol, 2016. 27(7): p. 1190–8. [PubMed: 26912558]
118. Samatov TR, et al. , Modelling the metastatic cascade by in vitro microfluidic platforms. Progress in Histochemistry and Cytochemistry, 2015. 49(4): p. 21–29. [PubMed: 25759320]
119. Sung KE, et al. , Transition to invasion in breast cancer: a microfluidic in vitro model enables examination of spatial and temporal effects. Integrative Biology, 2011. 3(4): p. 439–450. [PubMed: 21135965]
120. Liu T, et al. , A microfluidic device for characterizing the invasion of cancer cells in 3-D matrix. Electrophoresis, 2009. 30(24): p. 4285–4291. [PubMed: 20013914]
121. Zervantonakis IK, et al. , Three-dimensional microfluidic model for tumor cell intravasation and endothelial barrier function. Proceedings of the National Academy of Sciences, 2012. 109(34): p. 13515–13520.
122. Lee H, et al. , A microfluidic platform for quantitative analysis of cancer angiogenesis and intravasation. Biomicrofluidics, 2014. 8(5): p. 054102.
123. Shin MK, Kim SK, and Jung H, Integration of intra-and extravasation in one cell-based microfluidic chip for the study of cancer metastasis. Lab on a chip, 2011. 11(22): p. 3880–3887. [PubMed: 21975823]
124. Riahi R, et al. , A microfluidic model for organ-specific extravasation of circulating tumor cells. Biomicrofluidics, 2014. 8(2): p. 024103.
125. Stroock AD and Fischbach C, Microfluidic culture models of tumor angiogenesis. Tissue Engineering Part A, 2010. 16(7): p. 2143–2146. [PubMed: 20214470]

Author Manuscript Author Manuscript Author Manuscript Author Manuscript

126. Bischel LL, et al. , A microfluidic coculture and multiphoton FAD analysis assay provides insight into the influence of the bone microenvironment on prostate cancer cells. Integrative Biology, 2014. 6(6): p. 627–635. [PubMed: 24791272]

127. Wu J, Zheng G, and Lee LM, Optical imaging techniques in microfluidics and their applications. Lab on a Chip, 2012. 12(19): p. 3566–3575. [PubMed: 22878811]

128. Wirtz D, Konstantopoulos K, and Searson PC, The physics of cancer: the role of physical interactions and mechanical forces in metastasis. Nat Rev Cancer, 2011. 11(7): p. 512–22. [PubMed: 21701513]

129. Mei X, et al. , Microfluidic platform for studying osteocyte mechanoregulation of breast cancer bone metastasis. Integr Biol (Camb), 2019. 11(4): p. 119–129. [PubMed: 31125041]

130. Shupp AB, et al. , Cancer Metastases to Bone: Concepts, Mechanisms, and Interactions with Bone Osteoblasts. Cancers, 2018. 10(6): p. 182.

131. Sottnik JL and Keller ET, Understanding and targeting osteoclastic activity in prostate cancer bone metastases. Current molecular medicine, 2013. 13(4): p. 626–639. [PubMed: 23061677]

132. Krzeszinski JY, et al. , Lipid osteoclastokines regulate breast cancer bone metastasis. Endocrinology, 2017. 158(3): p. 477–489. [PubMed: 27967239]

133. Ryu J, et al. , Sphingosine 1-phosphate as a regulator of osteoclast differentiation and osteoclast–osteoblast coupling. The EMBO journal, 2006. 25(24): p. 5840–5851. [PubMed: 17124500]

134. Sarkar S, et al. , Sphingosine kinase 1 is required for migration, proliferation and survival of MCF-7 human breast cancer cells. FEBS letters, 2005. 579(24): p. 5313–5317. [PubMed: 16194537]

135. Kim E-S, et al. , Sphingosine 1-phosphate regulates matrix metalloproteinase-9 expression and breast cell invasion through S1P3–Gαq coupling. Journal of cell science, 2011. 124(13): p. 2220–2230. [PubMed: 21652634]

136. Oldstone MB and Rosen H, Sphingosine-1-phosphate signaling in immunology and infectious diseases. 2014: Springer.

137. Genetos DC, et al. , Oscillating fluid flow activation of gap junction hemichannels induces ATP release from MLO-Y4 osteocytes. Journal of cellular physiology, 2007. 212(1): p. 207–214. [PubMed: 17301958]

138. Zhou JZ, et al. , Differential impact of adenosine nucleotides released by osteocytes on breast cancer growth and bone metastasis. Oncogene, 2015. 34(14): p. 1831–1842. [PubMed: 24837364]

139. Jones DH, et al. , Regulation of cancer cell migration and bone metastasis by RANKL. Nature, 2006. 440(7084): p. 692–696. [PubMed: 16572175]

140. You L, et al. , Osteocytes as mechanosensors in the inhibition of bone resorption due to mechanical loading. Bone, 2008. 42(1): p. 172–179. [PubMed: 17997378]

141. Cheung W-Y, Simmons CA, and You L, Osteocyte apoptosis regulates osteoclast precursor adhesion via osteocytic IL-6 secretion and endothelial ICAM-1 expression. Bone, 2012. 50(1): p. 104–110. [PubMed: 21986000]

142. Ibrahim SA, et al. , Hormonal-receptor positive breast cancer: IL-6 augments invasion and lymph node metastasis via stimulating cathepsin B expression. Journal of Advanced Research, 2016. 7(5): p. 661–670. [PubMed: 27482469]

143. Heino TJ, Hentunen TA, and VaÈaÈnaÈnen HK, Osteocytes inhibit osteoclastic bone resorption through transforming growth factor-β: Enhancement by estrogen. Journal of cellular biochemistry, 2002. 85(1): p. 185–197. [PubMed: 11891862]

144. Itatsu K, et al. , Cyclooxygenase-2 is involved in the up-regulation of matrix metalloproteinase-9 in cholangiocarcinoma induced by tumor necrosis factor-α. The American journal of pathology, 2009. 174(3): p. 829–841. [PubMed: 19218340]

145. Nguyen DX, Bos PD, and Massagué J, Metastasis: from dissemination to organ-specific colonization. Nature Reviews Cancer, 2009. 9(4): p. 274–284. [PubMed: 19308067]

146. Paget S, The distribution of secondary growths in cancer of the breast. Lancet, 1889: p. 571–573.

147. Borenstein JT, et al., Three-dimensional microfluidic platforms and methods of use and manufacture thereof. 2011, Google Patents.

Author Manuscript Author Manuscript Author Manuscript Author Manuscript

148. Kamm RD, Chung S, and Vickerman-Kelley VV, Three-dimensional microfluidic platforms and methods of use thereof. 2015, Google Patents.

149. Koens R, et al. , Microfluidic platform for three-dimensional cell culture under spatiotemporal heterogeneity of oxygen tension. APL bioengineering, 2020. 4(1): p. 016106.

150. Kim S, et al. , Interstitial flow regulates the angiogenic response and phenotype of endothelial cells in a 3D culture model. Lab on a Chip, 2016. 16(21): p. 4189–4199. [PubMed: 27722679]

151. Bersini S, et al. , A combined microfluidic-transcriptomic approach to characterize the extravasation potential of cancer cells. Oncotarget, 2018. 9(90): p. 36110. [PubMed: 30546831]

152. Zhang M. and Sun J, Bone metastasis from ovarian cancer. Saudi Med J, 2013. 34(12): p. 1270–1273. [PubMed: 24343467]

153. Gentleman E, et al. , Comparative materials differences revealed in engineered bone as a function of cell-specific differentiation. Nature materials, 2009. 8(9): p. 763–770. [PubMed: 19633661]

154. Hao S, et al. , A Spontaneous 3D bone-on-a-chip for bone metastasis study of breast cancer cells. Small, 2018. 14(12): p. 1702787.

155. DiCostanzo D, et al. , Prognosis in infiltrating lobular carcinoma. An analysis of “classical” and variant tumors. Am J Surg Pathol, 1990. 14(1): p. 12–23. [PubMed: 2153007]

156. Ahn J, et al. , 3D Microfluidic Bone Tumor Microenvironment Comprised of Hydroxyapatite/Fibrin Composite. Frontiers in Bioengineering and Biotechnology, 2019. 7(168).

157. Jusoh N, et al. , Microfluidic vascularized bone tissue model with hydroxyapatite-incorporated extracellular matrix. Lab Chip, 2015. 15(20): p. 3984–8. [PubMed: 26288174]

158. Shi Z, et al. , Size effect of hydroxyapatite nanoparticles on proliferation and apoptosis of osteoblast-like cells. Acta Biomaterialia, 2009. 5(1): p. 338–345. [PubMed: 18753024]

159. Ducy P, Schinke T, and Karsenty G, The osteoblast: a sophisticated fibroblast under central surveillance. Science, 2000. 289(5484): p. 1501–1504. [PubMed: 10968779]

160. Miles FL, et al. , Stepping out of the flow: capillary extravasation in cancer metastasis. Clinical & experimental metastasis, 2008. 25(4): p. 305–324. [PubMed: 17906932]

161. Bersini S, et al. , A microfluidic 3D in vitro model for specificity of breast cancer metastasis to bone. Biomaterials, 2014. 35(8): p. 2454–2461. [PubMed: 24388382]

162. Gjerdrum C, et al. , Axl is an essential epithelial-to-mesenchymal transition-induced regulator of breast cancer metastasis and patient survival. Proceedings of the National Academy of Sciences, 2010. 107(3): p. 1124.

163. Hsu YL, et al. , Breast tumor-associated osteoblast-derived CXCL5 increases cancer progression by ERK/MSK1/Elk-1/Snail signaling pathway. Oncogene, 2013. 32(37): p. 4436–4447. [PubMed: 23045282]

164. Vuoriluoto K, et al. , Vimentin regulates EMT induction by Slug and oncogenic H-Ras and migration by governing Axl expression in breast cancer. Oncogene, 2011. 30(12): p. 1436–1448. [PubMed: 21057535]

165. Tikhonova AN, et al. , The bone marrow microenvironment at single-cell resolution. Nature, 2019. 569(7755): p. 222–228. [PubMed: 30971824]

166. Phuong ML, Michael A, and Venkata Lokesh B, Osteogenic niche in the regulation of normal hematopoiesis and leukemogenesis. Haematologica, 2018. 103(12): p. 1945–1955. [PubMed: 30337364]

167. Wei Q. and Frenette PS, Niches for hematopoietic stem cells and their progeny. Immunity, 2018. 48(4): p. 632–648. [PubMed: 29669248]

168. Morrison SJ and Scadden DT, The bone marrow niche for haematopoietic stem cells. Nature, 2014. 505(7483): p. 327–334. [PubMed: 24429631]

169. Carrion B, et al. , Recreating the perivascular niche ex vivo using a microfluidic approach. Biotechnology and bioengineering, 2010. 107(6): p. 1020–1028. [PubMed: 20672286]

170. Torisawa Y. s., et al. , Bone marrow–on–a–chip replicates hematopoietic niche physiology in vitro. Nature methods, 2014. 11(6): p. 663–669. [PubMed: 24793454]

171. Sieber S, et al. , Bone marrow-on-a-chip: Long-term culture of human haematopoietic stem cells in a three-dimensional microfluidic environment. Journal of tissue engineering and regenerative medicine, 2018. 12(2): p. 479–489. [PubMed: 28658717]

Author Manuscript Author Manuscript Author Manuscript Author Manuscript

172. Marturano-Kruik A, et al. , Human bone perivascular niche-on-a-chip for studying metastatic colonization. Proceedings of the National Academy of Sciences, 2018. 115(6): p. 1256–1261.

173. Aleman J, et al. , Deconstructed Microfluidic Bone Marrow On-A-Chip to Study Normal and Malignant Hemopoietic Cell–Niche Interactions. Small, 2019. 15(43): p. 1902971.

174. Chou DB, et al. , On-chip recapitulation of clinical bone marrow toxicities and patient-specific pathophysiology. Nature Biomedical Engineering, 2020. 4(4): p. 394–406.

175. Yokota H, Leong DJ, and Sun HB, Mechanical loading: bone remodeling and cartilage maintenance. Current osteoporosis reports, 2011. 9(4): p. 237. [PubMed: 21858507]

176. Chow J, et al. , Mechanical loading stimulates bone formation by reactivation of bone lining cells in 13-week-old rats. Journal of Bone and Mineral Research, 1998. 13(11): p. 1760–1767. [PubMed: 9797486]

177. Robinson JA, et al. , Wnt/β-catenin signaling is a normal physiological response to mechanical loading in bone. Journal of Biological Chemistry, 2006. 281(42): p. 31720–31728.

178. Lee KC and Lanyon LE, Mechanical loading influences bone mass through estrogen receptor α. Exercise and sport sciences reviews, 2004. 32(2): p. 64–68. [PubMed: 15064650]

179. Bonewald LF and Johnson ML, Osteocytes, mechanosensing and Wnt signaling. Bone, 2008. 42(4): p. 606–615. [PubMed: 18280232]

180. Stevens MM, Biomaterials for bone tissue engineering. Materials today, 2008. 11(5): p. 18–25.

181. Gao C, et al. , Bone biomaterials and interactions with stem cells. Bone research, 2017. 5(1): p. 1–33.

182. Thrivikraman G, et al. , Biomaterials for craniofacial bone regeneration. Dental Clinics, 2017. 61(4): p. 835–856. [PubMed: 28886771]

183. Liu M, et al. , Injectable hydrogels for cartilage and bone tissue engineering. Bone research, 2017. 5(1): p. 1–20.

184. Reznikov N, Shahar R, and Weiner S, Bone hierarchical structure in three dimensions. Acta Biomaterialia, 2014. 10(9): p. 3815–3826. [PubMed: 24914825]

185. Noori A, et al. , A review of fibrin and fibrin composites for bone tissue engineering. International journal of nanomedicine, 2017. 12: p. 4937. [PubMed: 28761338]

186. Breen A, O'Brien T, and Pandit A, Fibrin as a delivery system for therapeutic drugs and biomolecules. Tissue Engineering Part B: Reviews, 2009. 15(2): p. 201–214.

187. Park YK, et al. , In vitro microvessel growth and remodeling within a three-dimensional microfluidic environment. Cellular and molecular bioengineering, 2014. 7(1): p. 15–25. [PubMed: 24660039]

188. Thrivikraman G, et al. , Rapid fabrication of vascularized and innervated cell-laden bone models with biomimetic intrafibrillar collagen mineralization. Nature Communications, 2019. 10(1): p. 3520.

189. He F, et al. , Multiscale characterization of the mineral phase at skeletal sites of breast cancer metastasis. Proceedings of the National Academy of Sciences, 2017. 114(40): p. 10542.

190. De Yoreo JJ and Sommerdijk NA, Investigating materials formation with liquid-phase and cryogenic TEM. Nature Reviews Materials, 2016. 1(8): p. 1–18.

191. Novak R, et al. , Robotic fluidic coupling and interrogation of multiple vascularized organ chips. Nature Biomedical Engineering, 2020. 4(4): p. 407–420.

192. Herland A, et al. , Quantitative prediction of human pharmacokinetic responses to drugs via fluidically coupled vascularized organ chips. Nature Biomedical Engineering, 2020. 4(4): p. 421–436.

Author Manuscript
Author Manuscript
Author Manuscript
Author Manuscript

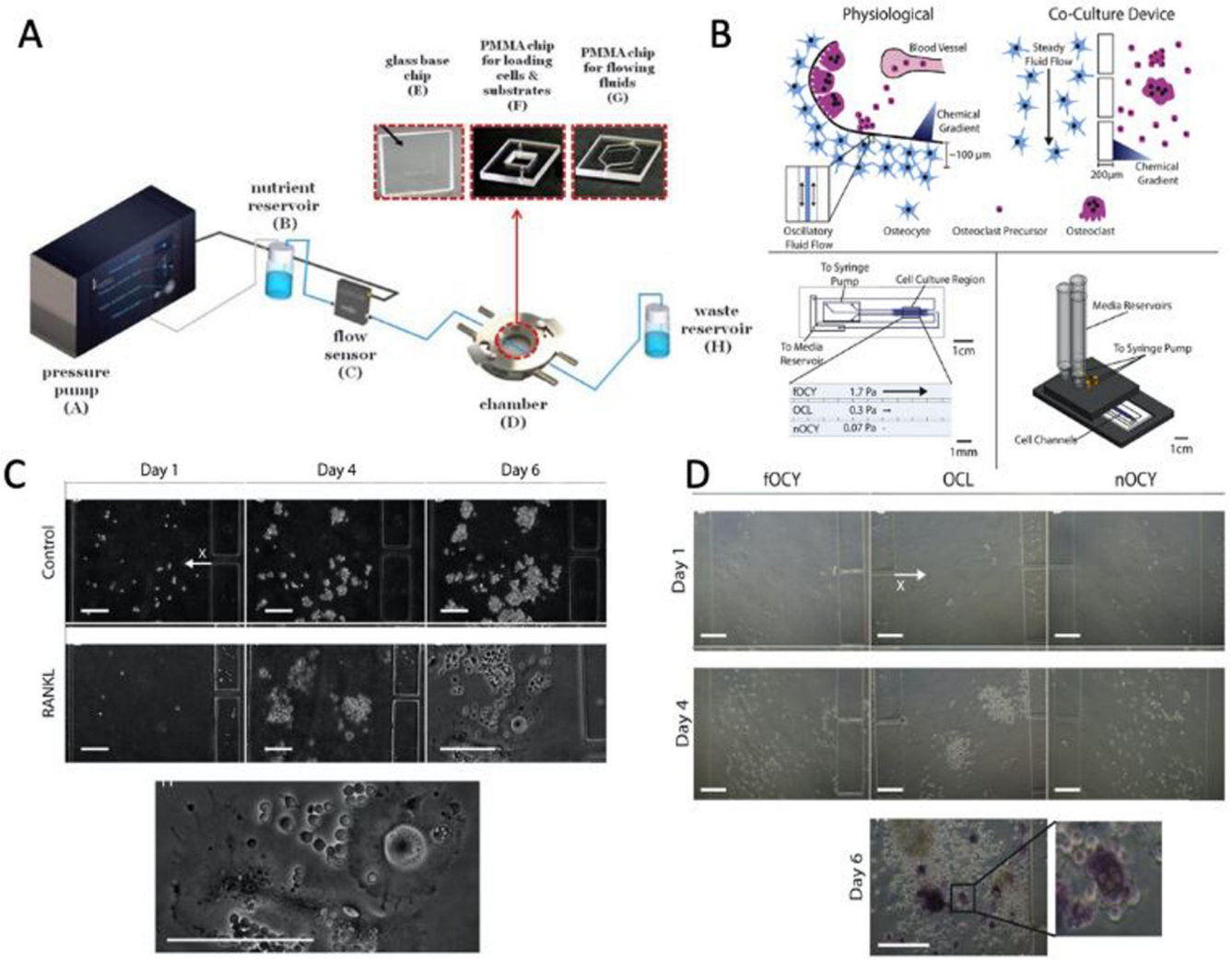

Figure 1.

A) Illustration of the microfluidic system composed of a high precision pressure pump, nutrient and waste reservoirs, flow sensor, and the microfluidic chamber is shown. B) The schematic shows a comparison between the physiological environment and how the microfluidic device is employed to mimic this environment as well as how the microfluidic device is mounted on a manifold. C) Images of negative control media and RANKL supplemented media after 1, 4, and 6 days of culture. The bottom image shows a magnified image of osteoclasts in RANKL supplemented media after 6 days. Scale bars are 200 µm. D) Images of the cells in fOCY (stimulated osteocytes channel), OCL (osteoclasts channel), and nOCY (non-stimulated osteocytes channel) channels after 1 and 4 days of culture. The bottom image shows the TRAP+ staining of osteoclasts on day 6 of co-culture. The zoomed view clearly shows the multinucleated osteoclasts. Scale bars are 200 µm. (Adapted under the terms of the CC-BY license.[64] 2018, MDPI. Adapted with permission.[72] 2017, Elsevier.)

Author Manuscript Author Manuscript Author Manuscript Author Manuscript

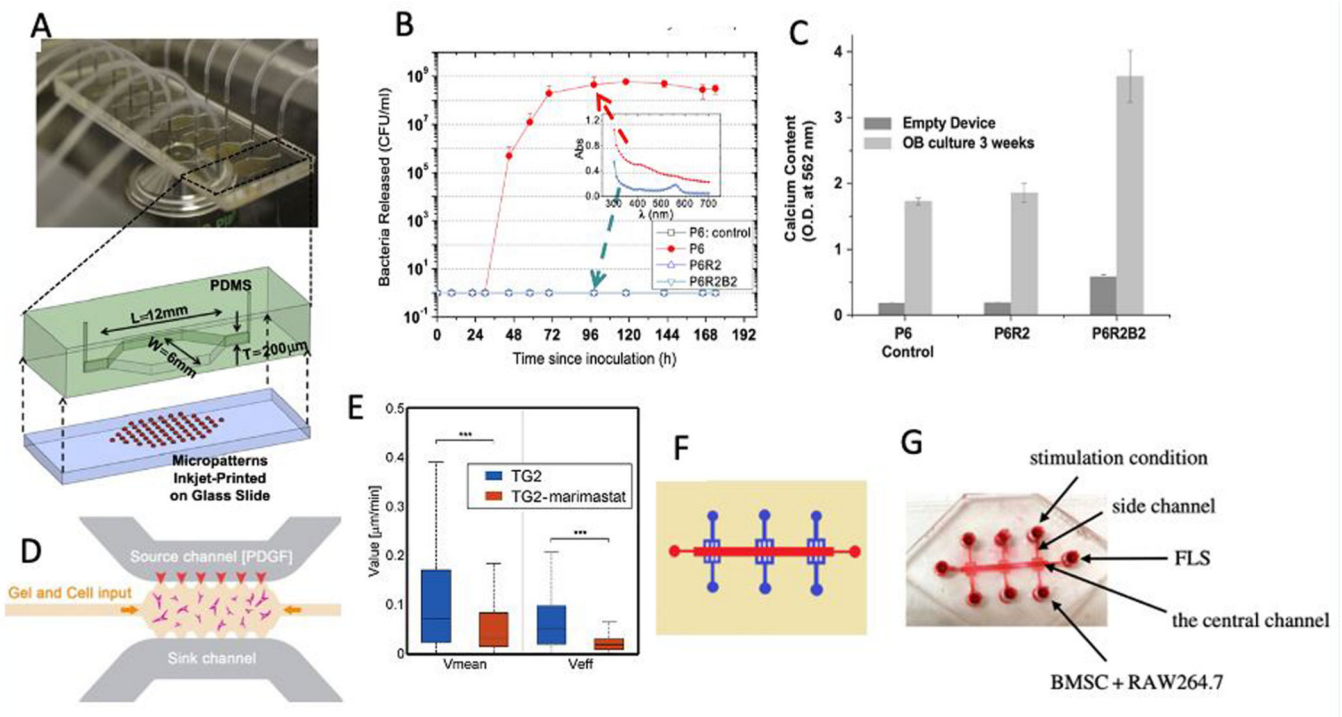

Figure 2.

A) A high-throughput microfluidic system with 8 culture chambers integrated with inkjet-printed micropatterns and an exploded view of an individual chamber are shown. B) Using micropatterns containing RFP antibiotics decreased the S. epidermis bacteria released in the microfluidic chamber. The inset shows the UV-VIS absorption spectra of the effluents at 96 h. C) The presence of micropatterns after a 3-week co-culture increased the calcium deposition. D) One of the side channels of the microfluidic system was filled with PDGF containing media to create a concentration gradient across the gel channel to mimic the bone injury or fraction. E) Median and effective velocities of osteoblasts decreased by adding Marimastat MMP inhibitor. F) The schematic of the microfluidic device for studying FLS migration is shown. G) In order to mimic FLS migration in RA, human synovium SW982 cells were cultured in the central channel, while RAW264.7 RANKL stimulated and osteogenic medium stimulated BMSCs were cultured on the side chamber. (Adapted with permission.[82] 2012, Elsevier. Adapted with permission.[86] 2018, Elsevier. Adapted under the terms of the CC-BY license.[90] 2018, The Royal Society Publishing)

Author Manuscript Author Manuscript Author Manuscript Author Manuscript

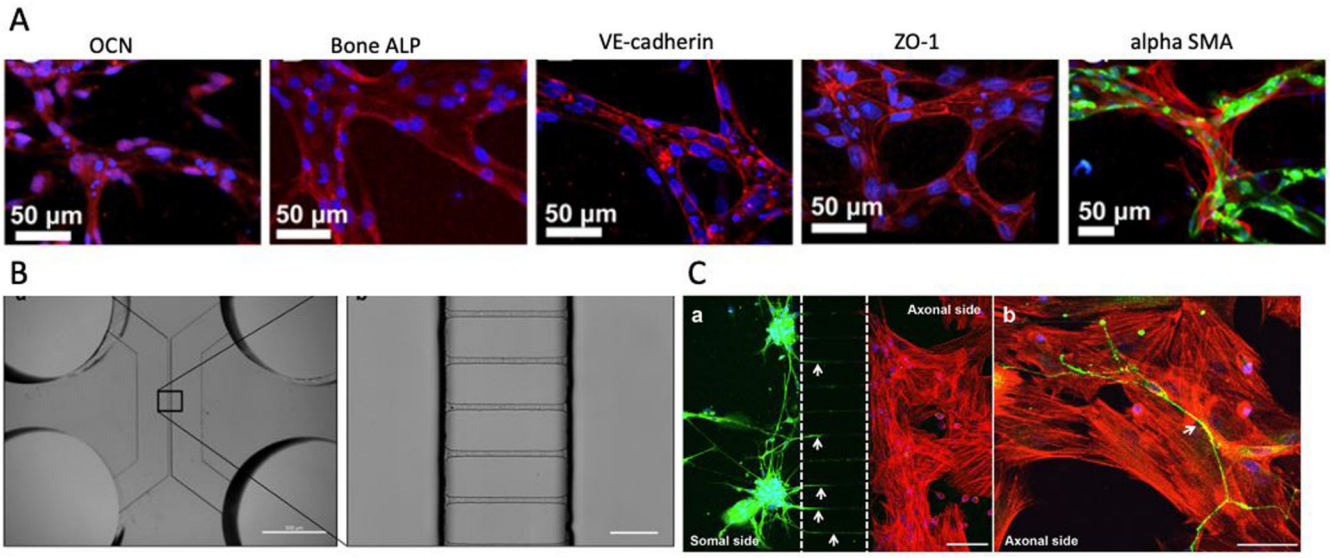

Figure 3.

A) Formation of bone and the microvascular network is confirmed by staining for osteocalcin (OCN red), bone ALP (Bone ALP red), endothelial adherens (VE-cadherin red), and tight junctions (ZO-1 red). Furthermore, differentiation of hBM-MSCs toward mural cell lineage is confirmed by immunofluorescent staining of alpha-smooth muscle actin (alpha SMA red). HUVECs and nucleus are stained with green and DAPI (blue) stainings, respectively. B) A microscopic image of the microfluidic device for studying innervation and a zoomed view at microgrooves is shown. The microgrooves are 3.6 µm high, 7 µm wide, and 148 µm long, which are spaced 48 µm from one another. Scale bar is 10 µm. C) The presence of neurites after co-culture with MSCs using the microfluidic device is evident in this image. Immunofluorescent staining of neurites was performed using ß-III Tubulin coupled to Alexa Fluor 488 (green), and the nuclei were stained with DAPI. Alexa Fluor 568 (red)-conjugated phalloidin was used for staining MSCs' actin filaments. The scale bars are 100 µm and 50 µm from left to right, respectively. (Adapted under the terms of the CC-BY license.[106] 2014, Proceedings of the National Academy of Sciences of the United States of America. Adapted under the terms of the CC-BY license.[112] 2017, Nature Publishing Group.)

Author Manuscript Author Manuscript Author Manuscript Author Manuscript

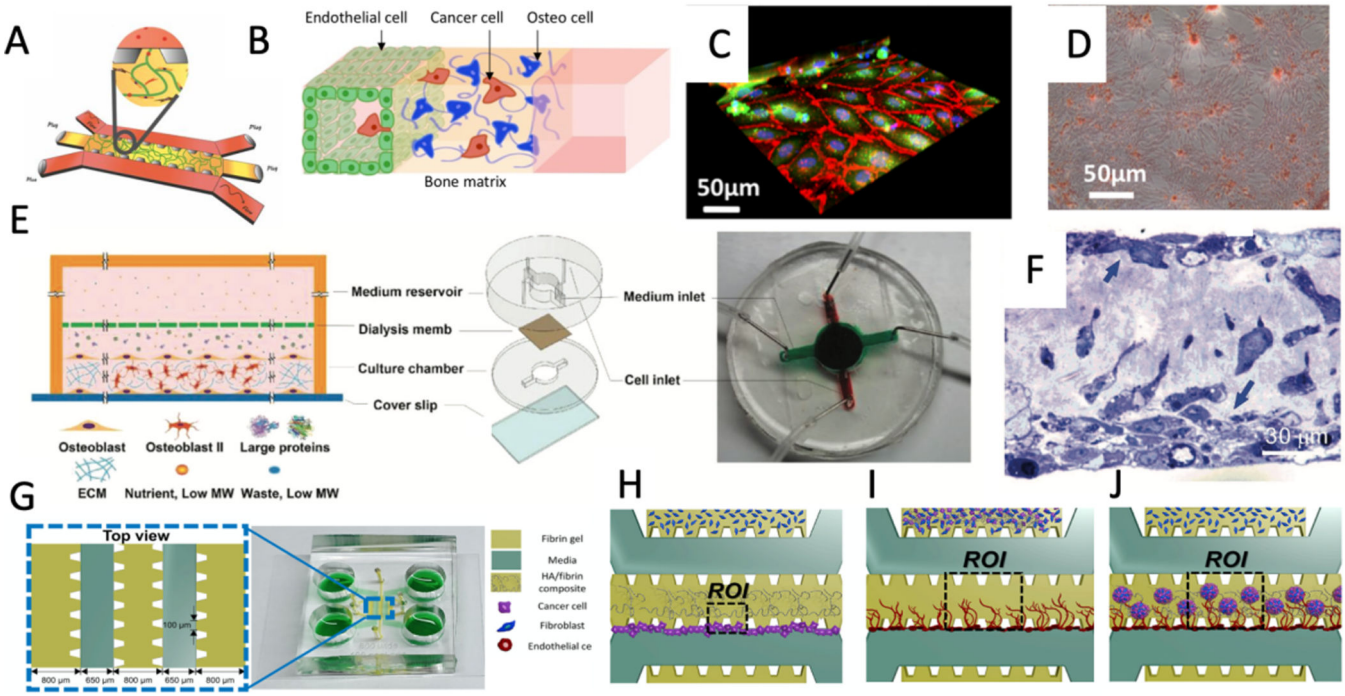

Figure 4.

A) The microfluidic device developed by Roger Kamm's group that has been widely used in organ-on-a-chip devices. B) A schematic of a tri-culture microfluidic device to study cancer cell extravasation through endothelial lumen and ECM. C) 3D reconstruction of VE-cadherins (red) showing the formation of adherens junctions between GFP endothelial cells, while cell nuclei are shown in blue (Hoechst) D) deposition of calcium deposited by MSCs shown by Alizarin Red-S assay E) Schematic and image of the microfluidic device used to obtain a mature osteoblastic tissue over 30 days. In this device, culture and medium reservoirs are separated by a dialysis membrane to increase the efficiency of nutrients and waste exchange as well as trapping the bone-building proteins. F) Horizontal view of the toluidine stained osteoblastic tissue formed after 30 days shows apical and basal layers of osteoblasts. G) Schematic and image of three gel channels microfluidic device for studying mineralized bone tissue made of HA/fibrin composite. Representation of cells and ECM configuration for studying the effects of HA concentration on H) extravasation, I) tumor-induced microenvironment angiogenesis, and J) crosstalk between tumor and tumor microenvironment. (Adapted under the terms of the CC-BY license.[151] 2018, Impact Journals. Adapted with permission.[154] 2018, Wiley. Adapted under the terms of the CC-BY license.[156] 2019, Frontiers.)

Author Manuscript Author Manuscript Author Manuscript Author Manuscript

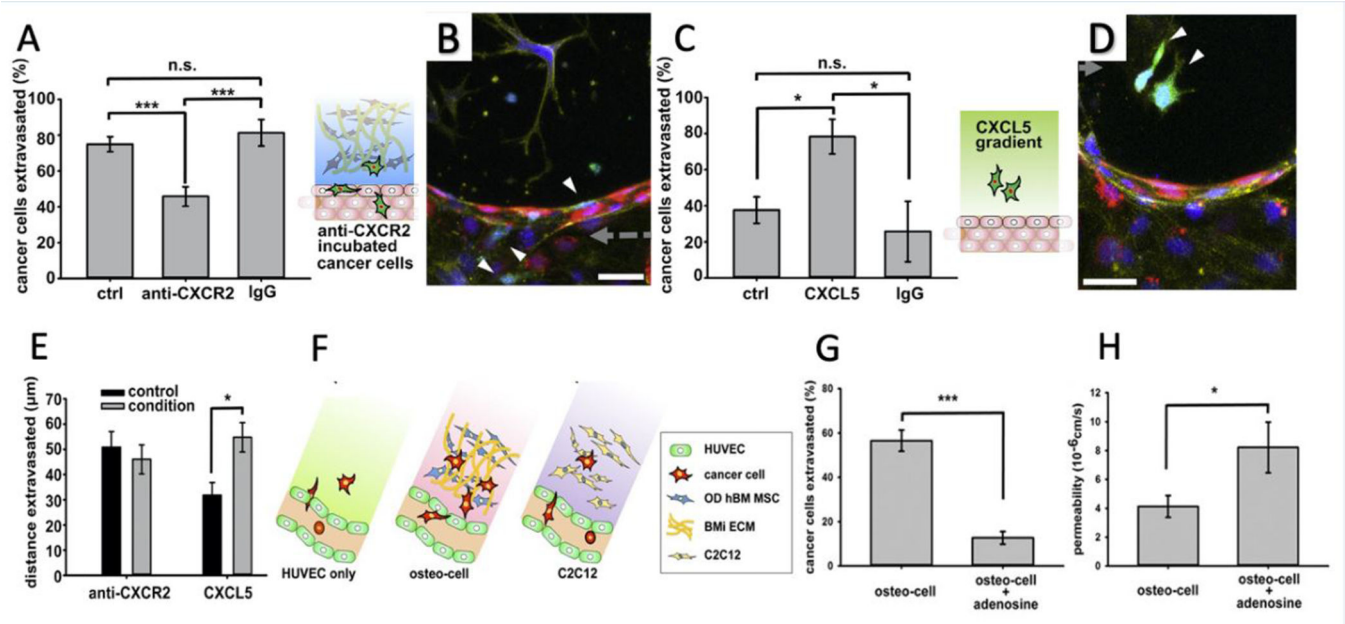

Figure 5.

A) Treating cancer cells with CXCR2 blocking antibody decreased the extravasation rate of cancer cells within collagen gel containing OD hBM-MSCs compared to non-treated and IgG incubated cancer cells. B) confocal stack image of non-extravasated anti-CXCR2 treated cancer cells (GFP, white arrows) into the gel.cells nucleus, endothelial cells, and actin filaments are stained with DAPI (blue), RFP (red), and phalloidin (yellow), respectively. C) addition of CXCL5 within collagen gel-only increased the extravasation rate of cancer cells compared to non-treated, and IgG added collagen gels. D) Confocal stack image of extravasated cancer cells to the collagen gel. Similarly, cell nucleus, endothelial cells, and actin filaments are stained with DAPI (blue), RFP (red), and phalloidin (yellow), respectively. E) Incubating cancer cells with the CXCR2 blocking antibody did not affect the extravasation distance while treating collagen gel with CXCL5 decreased extravasation distance. F) C2C12 or OD hBM-MSC cells could be used to mimic bone and muscle microenvironments, respectively. G) Percentage of cancer cells extravasated with adding adenosine decreased. H) On the other hand, adding adenosine increased the permeability of the microenvironment. (Adapted with permission.[161] 2014, Elsevier. Adapted under the terms of the CC-BY license.[106] 2015, Proceedings of the National Academy of Sciences of the United States of America.)

Author Manuscript Author Manuscript Author Manuscript Author Manuscript

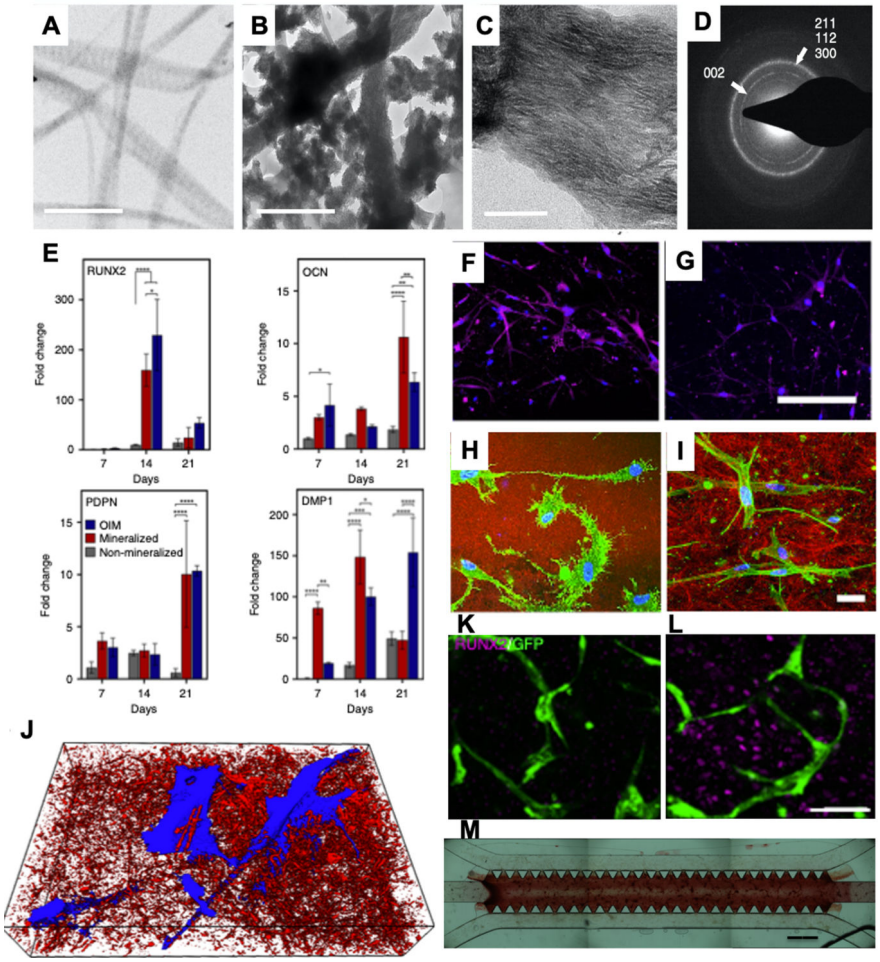

Figure 6.

TEM image of A) non-mineralized and B) mineralized collagen shows the formation of intra and extrafibrillar mineralization in the mineralized sample (scale bar: 500 nm). C) Zoomed TEM view of the mineralized sample shows the orientation of intrafibrillar mineral apatite crystallites in (001) position (scale bar: 50 nm). D) Selective area electron diffraction (SAED) shows the broad arc for (002) plane and overlapping arcs for (112), (211), and (300) planes similar to hydroxyapatite crystalline structure. E) Cells in the mineralized matrix showed higher or comparable gene expression profiles to those obtained by OIM, with the exception of RUNX2. The expression of OCN on day 14 in the F) mineralized sample was significantly higher compared to the OIM-treated sample (purple: OPN, blue: DAPI, scale bar: 200 μm). Reflectance confocal microscopy of MSCs in H) mineralized and I) OIM-treated samples shows the dendritic morphology of cells in the mineralized sample, indicating an osteocyte-like morphology (green: F-actin, blue: DAPI, red: collagen, scale bar: 30 μm). J) 3D SEM image of cells (blue) packed in minerals (red). Comparing HUVECs:MSCs co-culture in K) non-mineralized and L) mineralized samples shows the expression of RUNX2 by MSCs as a marker for osteogenic differentiation (scale bar: 50 μm). M) The proposed mineralization method was used in the microfluidic device seeded with HUVECs:MSCs co-cultured in collagen:fibrin gel, and the Alizarin red data showed the

mineralization and deposition of calcium in the vascularized microfluidic model. (Adapted under the terms of the CC-BY license.[188] 2019, Nature Publishing Group)

Author Manuscript Author Manuscript Author Manuscript Author Manuscript